IDEA

Innovations Deserving Exploratory Analysis Programs

NCHRP IDEA Program

A Real-Time Proactive Intersection Safety Monitoring and Visualization System Based on Radar Sensor Data

Final Report for
NCHRP IDEA Project 217

Prepared by:
Zhixia (Richard) Li
Muting Ma, Ph.D.
University of Louisville

April 2022

NATIONAL ACADEMIES Sciences Engineering Medicine

TRB TRANSPORTATION RESEARCH BOARD

Innovations Deserving Exploratory Analysis (IDEA) Programs Managed by the Transportation Research Board

This IDEA project was funded by the NCHRP IDEA Program.

The TRB currently manages the following three IDEA programs:

- The NCHRP IDEA Program, which focuses on advances in the design, construction, and maintenance of highway systems, is funded by American Association of State Highway and Transportation Officials (AASHTO) as part of the National Cooperative Highway Research Program (NCHRP).
- The Safety IDEA Program currently focuses on innovative approaches for improving railroad safety or performance. The program is currently funded by the Federal Railroad Administration (FRA). The program was previously jointly funded by the Federal Motor Carrier Safety Administration (FMCSA) and the FRA.
- The Transit IDEA Program, which supports development and testing of innovative concepts and methods for advancing transit practice, is funded by the Federal Transit Administration (FTA) as part of the Transit Cooperative Research Program (TCRP).

Management of the three IDEA programs is coordinated to promote the development and testing of innovative concepts, methods, and technologies.

For information on the IDEA programs, check the IDEA website (www.trb.org/idea). For questions, contact the IDEA programs office by telephone at (202) 334-3310.

IDEA Programs
Transportation Research Board
500 Fifth Street, NW
Washington, DC 20001

A Real-Time Proactive Intersection Safety Monitoring and Visualization System Based on Radar Sensor Data

IDEA Program Final Report

Project 217

Prepared for the IDEA Program

Transportation Research Board

The National Academies

Zhixia (Richard) Li, Principal Investigator

and

Muting Ma, Ph.D.

Center for Transportation Innovation

University of Louisville

ACKNOWLEDGMENTS

The authors express appreciation to the following individuals who contributed to the program. We sincerely thank Dr. Emily Parkany and Dr. Paul Carlson as advisors for guiding the project and Mr. Mike Vaughn, Mr. Jarrod Stanley, and Mr. Dirk Gowin as the expert panel for providing expert comments and suggestions to improve the product. Special thanks go to Dr. Song Wang, Mr. Majeed Algomaiah, Mr. Yingfan Gu, Mr. Taoran Li, and especially engineering technician Bernie Miles for assisting with the data collection. Lastly, we appreciate Dr. Inam Jawed for his guidance and comments on project management.

EXPERT REVIEW PANEL
Emily Parkany, *Vermont AOT*
Paul Carlson, *Automated Roads*
Michael Vaughn, *Kentucky Transportation Cabinet*
Jarrod Stanley, *Kentucky Transportation Cabinet*
Dirk Gowin, *City of Louisville*

TABLE OF CONTENTS

EXECUTIVE SUMMARY

Aiming to provide a safe driving environment, transportation agencies have begun monitoring traffic flow, collecting traffic data, and conducting safety analyses by using proactive roadside sensing technologies for decades. These sensing technologies consist of radar sensors, Lidar, and video cameras. However, those safety analyses at an intersection are restricted by a limited data collection time or specific conflict types in a specific traffic scenario. Consistent data collection requires consistent power supplies and/or manual operations and maintenance. In addition, a data processing algorithm in a safety analysis system is developed for only a specific conflict scenario. These restrictions prevent transportation agencies from widely deploying safety applications at any targeted intersection for long-term monitoring. To overcome such limitations, this IDEA product developed a proactive intersection safety monitoring and visualization system that can be implemented at any kind of intersection for any type of safety and operation analysis under a long-term data collection period. The product's contributions, Intersection Proactive Safety Visualization (IPSV), can be summarized as follows.

Innovation

First, in contrast to other traffic detection products, such as using video cameras, drones, or Lidar sensors, the IPSV employs a 24GHz Microwave Doppler radar sensor, which can detect an object by the frequency difference received between the transmitted and reflected waveform and log the trajectory points with frequency up to 0.3 s/point. As long as the object moves with a speed of at least 0.62 cm/s the Doppler radar used in the IPSV can detect and track its trajectory of it. In addition, the data storage for the detected trajectories using a radar sensor is minimal in comparison with using a video camera; the latter does not only require significant data storage and computational power if 24/7 monitoring is performed but also relies on complicated algorithms to track objects' maneuver if the aforementioned range resolution and accuracy is targeted. Moreover, the radar sensor is immune to the inclement weather and interference of light, whereas this characteristic is not available for other products on the market.

Second, the IPSV provides safety analyses in terms of traffic conflicts detected at the intersection. These conflict types include rear-end/lane-change/left-turn angle/right-angle/sideswipe/pedestrian-to-vehicle conflicts. The IPSV can be used at either signalized or stop-controlled intersections. Most IPSV functions are made automated with limited manual configurations. Besides, the conflicts are visualized symmetrically on the intersection satellite map and classified by any identifiers of TTC, movements, or conflict types to supplement the information to transportation agencies to facilitate identifying intersection safety issues that are difficult to be discovered by historical crash data. Furthermore, an application interface is developed along with the IPSV for users to make customized queries, analyses, and visualizations.

In addition to the IPSV development, two field data collections were conducted to validate the results of the IPSV. Through validating the results from the perspective of conflict severity and quantity of different conflict types, the IPSV system is upgraded from Stage 1 to Stage 2 by fixing the algorithm problems identified in Stage 1 and making the system more automated and integrated. Finally, the IPSV system upgraded in Stage 2 achieves a high conflict severity detection accuracy with an average 4.8% error rate. The system also achieves an 80% true positive rate and a 100% true negative rate for conflict quantity detection. The results are validated through manual comparisons of ground truth found in videos.

Furthermore, a data collection manual and a series of tutorial videos are created for deploying the IPSV system at an intersection. A system manual consisting of data collection devices, field calibration, installation methods, and maintenance procedures are readily utilized for transportation agencies to widely deploy the IPSV at more targeted intersections.

Results

In terms of safety issue visualization, the IPSV provides conflict severity distribution visualization by TTC value, the speed difference between conflicting objects, and any conflict/movement type. From the visualization, more dangerous spots where conflicts occur can be identified at an intersection, i.e., the conflict hot spots can be exactly targeted at a satellite map of the intersection.

In terms of safety issue monitoring, the IPSV also provides conflict quantity analyses categorized by time, TTC range, and traffic volume. During different times in a day, the variance of the conflict quantity of different conflict types can be obtained from the system.

In terms of decision-making on safety improvement at an intersection, the IPSV works as a fundamental platform for identifying safety issues of any intersections. Two signalized intersections were selected as the test intersection in Stage 1, where several conflicts of rear-end type are more than crossing type and illegal left turn and red light running were observed. A stop-controlled intersection was selected in Stage 2, where several conflicts of crossing type are more than rear-end type, and conflicts of pedestrian-to-vehicle are mostly observed. Overall, the IPSV can identify corresponding safety problems regarding different types of intersections.

Future Work

The first challenge that is learned from the development is that positioning errors caused by windy conditions can lead to less accurate TTC measurements and false or missed conflict detections. The positioning errors during windy conditions was not anticipated in Stage 1, as this error was discovered through field test in Stage 1. In general, positioning errors occur for any types of sensors deployed for data collection, including GPS, Lidar, and video cameras. Such positioning errors, however, can be mostly eliminated by post-processing algorithms. Such post-processing algorithms have been developed and implemented in Stage 2 of this project and have improved the accuracy.

The second challenge comes from the calibration of the trajectory of IPSV with the ground-truth trajectory data. It costs huge labor work to obtain the ground truth trajectories from videos. Because the greater number of ground truth is retrieved, the more accurate the calibration is and so is the conflict severity. More labor calibrations are recommended for better conflict detection results.

The third challenge arises in radar sensors' field data collection and calibration. For a radar sensor set up at a lighting pole, it is important to avoid any blockage within the detection width of the radar sensor; otherwise, the data becomes unreliable. In addition, a continuous trajectory rather than discrete trajectory points is recommended for visualization in the field of radar sensor angle calibration.

1. IDEA PRODUCT

This project develops and tests a real-time intersection proactive safety visualization (IPSV) system based on radar sensors' vehicle and pedestrian trajectory data. The IPSV algorithm is based on the automated collection of radar sensor data. Vehicle trajectory data is collected from radar sensors installed at an intersection. The IPSV involves an automated data preprocessing algorithm. The algorithm integrates trajectory data from four radar sensors at the intersection. A noise reduction module was developed in the algorithm to remove trajectory noise from the analysis. In addition, a coordinate transformation and trajectory data integration module was implemented in the algorithm to combine trajectory data from the four radar sensors in the same reference coordinate system. A second algorithm that automatically classifies different traffic and pedestrian movements was developed to enable automatic computing of time to different types of collision. The algorithm finally identifies conflicting traffic/pedestrian movements. Based on predefined thresholds of time to collision (TTC), in which 1.5 s and 4 s were tentatively used for identifying, respectively, rear-end and crossing conflicts, traffic conflicts of different types, and their severities were automatically identified and measured. Traffic safety events such as illegal left turns, wrong-way driving, and pedestrian jaywalking are also identified by the IPSV. The IPSV has a user interface to configure parameters. The IPSV also maps and visualizes the traffic conflicts with different servers, as represented by TTC and speeds.

2. CONCEPT AND INNOVATION

Intersection crashes constitute a significant portion of total crashes nationwide, which amount to about 44 percent of all reported crashes. If only considering fatal and injury crashes, The Federal Highway Administration reported that more than 50 percent of the combined total of fatal and injury crashes occur at or near intersections. Therefore, to improve highway safety, it is imperative to target the intersection with priority via long-term and short-term safety treatment strategies, considering that the majority of crashes happen at intersections. During any intersection safety treatment process, understanding what the typical safety issues are, how frequent they happen, and how severe are, are the key to the success of an effective, right-on-the-point treatment. In this sense, appropriate visualization of a safety problem at intersections is the essential first step toward developing the ultimate safety treatment solutions. Traditional methods of this type of visualization include (1) an intersection collision diagram and (2) and GIS-based intersection crash hot spot map. Figure 1 illustrates these two types of intersection safety issue visualization.

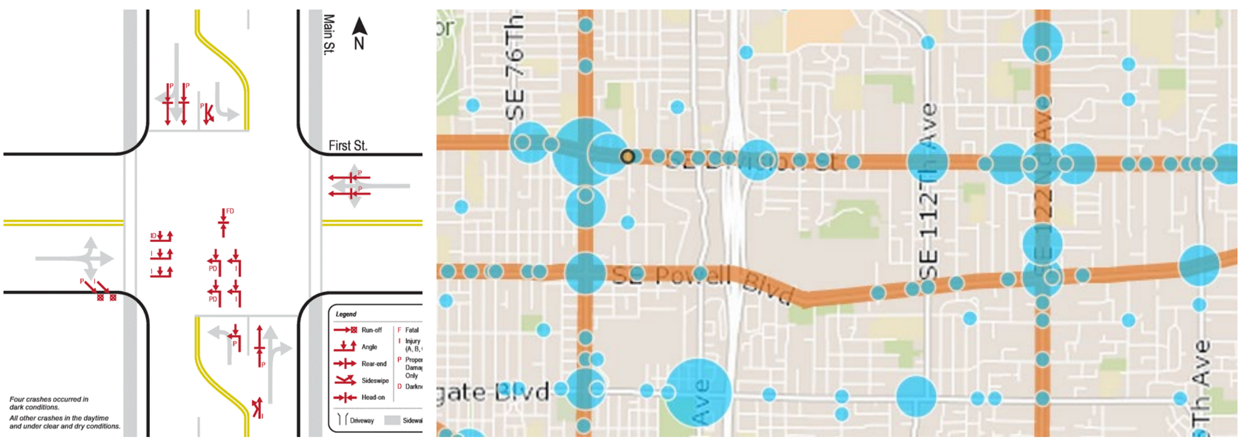

(a) (b)

FIGURE 1 Traditional approaches for intersection safety visualization: (a) intersection collision diagram, and (b) GIS-based intersection crash hot spot map.

Because all these methods are based on historical crash data, the user of such data must wait until crashes to happen to create such collision diagrams and intersection crash hot spot maps. However, such **reactive** methods hinder transportation agencies from effectively monitoring and visualizing safety issues. To overcome the limitations, the traffic conflict technique has been advocated as a **proactive** approach to studying traffic safety from a broader perspective than relying only on crash data analysis (*1, 2*). A traffic conflict is defined as "an observable situation in which two or more road users approach each other in space and time to such an extent that there is a risk of collision if their movements remained unchanged" (*3*). Since traffic conflicts are easily observant, several conflict detection methods have been developed to provide a better representation of traffic situations through radar sensor data (*4-9*), video data (*10-17*), or Lidar data (*18, 19*) in real time.

As a wealth of 'big data' can be utilized nowadays, data that can provides the most effective predictions and insights for policymakers to arrive at solutions in a timely fashion is needed. The potential data sources such as video data, drone data, Waze data, and social media data, are obtained either based on long-time training (video data), manual control (drone data), user-oriented trigger mechanism (Waze data), or data scraping (social media data). These data is valuable in terms of high-resolution observation and local incidents identification. However, for 24/7 continuously monitoring and preventing traffic safety issues, these mentioned data sources are not capable of meeting the requirements of real-time. Radar sensor data is widely used, validated, and proved to be alternatively advanced data in terms of stability, reliability, and privacy (*4-6*). Using this data source, 24/365 traffic safety enhancement becomes a reality. Furthermore, by using surrogate safety measures, such as Time-to-collision (TTC), the proactive intersection safety issues can be qualitatively and quantitively monitored and visualized. TTC is defined as the expected time for two vehicles to collide if they remain at their present speed and on the same path (*20*).

The real-time proactive intersection safety monitoring and visualization system is illustrated in **FIGURE** *2*. The uniqueness of the developed system, IPSV, can be demonstrated as follows:

1. Provides a cost-effective method to quickly evaluate safety treatment effectiveness for an intersection without the need of waiting crashes to happen; This method has potential to provide such quick evaluation as TTC and traffic conflicts resulted from IPSV will be used as surrogate safety measures to represent the likelihood of a crash to happen. If the TTC is less than the threshold, a traffic conflict exists. The probability for a traffic conflict to become a real accident is about 0.0001 (*35*).
2. Complements the crash data to help transportation agencies and local government better understand the safety issues at an intersection with traffic conflicts data collected;

3. Recognizes wide ranges of road users including vehicles, bicyclists, and pedestrians via an explainable feature-based algorithm;
4. Detects traffic anomaly consisting of detecting illegal left-turns, jaywalkers, and red-light-runners in any desired observation period;
5. Visualizes conflicts severity and quantity straightforwardly with the identifiers of TTC, vehicle speed, movements, or conflict types;
6. Applies to any type/number/geometry shape of lanes of an approach at an intersection by an automated and integrated system;
7. Performs real-time feedback about target intersection safety issues with consecutive 24/7 traffic monitoring.

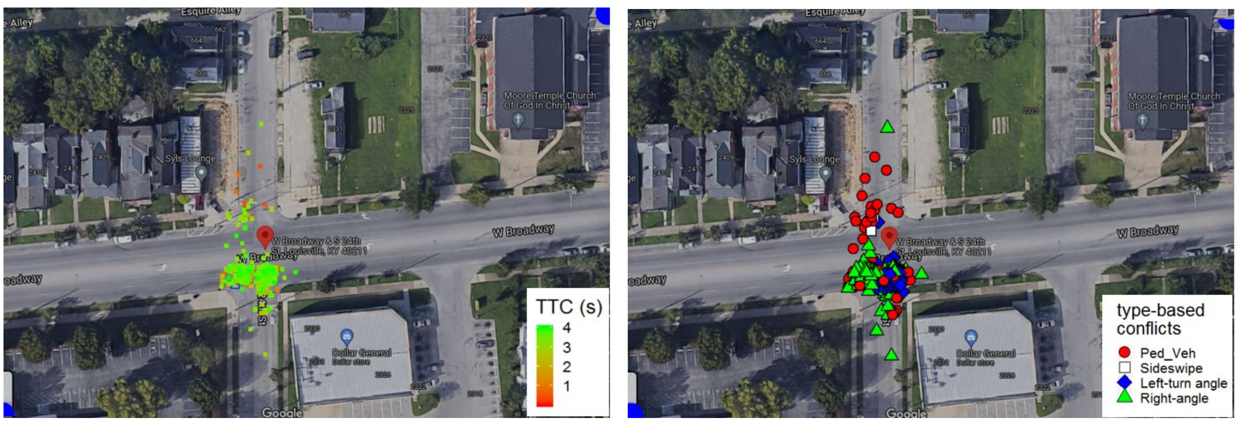

(a) (b)

FIGURE 2 Real-time proactive intersection safety monitoring and visualization: (a) TTC-based conflict distribution and (b) type-based conflict distribution.

3. INTERSECTION PROACTIVE SAFETY VISUALIZATION (IPSV) DEVELOPMENT IN STAGE 1

3.1 **ACCOMPLISHMENTS DURING THIS STAGE**

- Development of the automated data preprocessing algorithm that includes trajectory noise removal module and coordinate transformation and radar data integration module;
- Development of the algorithm of automated traffic movement classification and time-to-collision and traffic conflicts computation;
- Field radar data collection at two closely spaced urban signalized intersections in Louisville, Kentucky to evaluate the safety of these intersections, and at the same time use the data to prove the concept of the IPSV algorithm.

3.2 **WORK PERFORMED IN THIS STAGE**

3.2.1 Development of the Automated Data Preprocessing Algorithm

3.2.1.1 Trajectory Noise Removal Module

A trajectory noise removal module for IPSV was developed to remove noise from the trajectory data collected by radar sensors. The radar sensor can detect all moving objects' trajectories up to 600 feet from the radar sensor within a 30-degree detection zone. **FIGURE *3*** illustrates the detection zones of radars used in the IPSV system. Noise that represents trajectories of pedestrians, vehicles, or other moving objects that are not within the travel lanes, crosswalks, or sidewalks needs to be removed.

FIGURE 3 Detection zone of radars in the IPSV system.

FIGURE *4* (a) illustrates the raw trajectory data collected by a radar sensor. As shown in **FIGURE** *4* (a), the noise (marked by red circles) is neither on travel lanes, crosswalks, or sidewalks. A trajectory noise removal module for IPSV was developed to automatically remove the noise based on the known coordinates of the travel lane, crosswalk, and sidewalk boundaries. **FIGURE** *4* (b) illustrates the processed raw trajectory data with noise being removed.

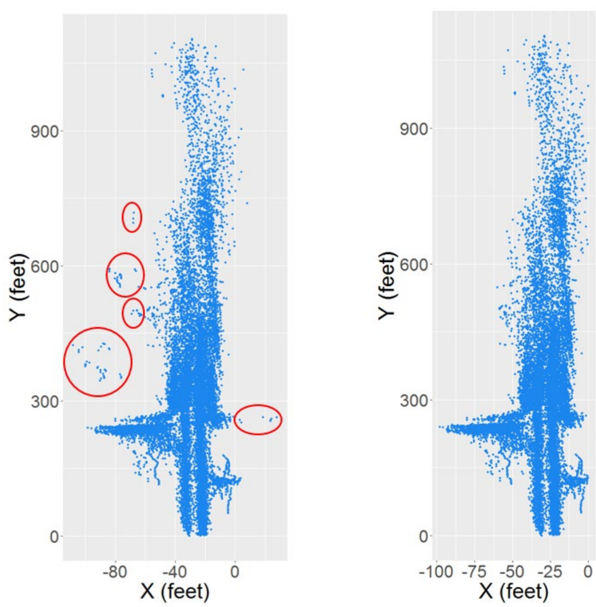

(a) (b)

FIGURE 4 Trajectory noise removal: (a) raw trajectory data; (b) process raw trajectory data after noise is removed.

3.2.1.2 Coordinate Transformation Module and Radar Data Integration Module

A coordinate transformation and radar data integration module for IPSV was developed, which combines trajectory data from multiple radar sensors covering different approaches to the intersection. Specifically, a module to combine all processed raw data from different radars was developed through coordinate transformation, as the processed raw data from each radar is in its own coordinate system. Therefore, the coordinate system of each radar sensor's processed raw data needs to be transformed into a reference coordinate system to combine all radar sensors' data in the same coordinate system. The coordinate transformation module involves two steps.

Step 1: Tilt angle rotation: There is an angle between the radar's center beam and the center line of the intersection approach where the radar is facing. In the coordinate system of the processed raw trajectory data, this angle tilts the trajectory data on that intersection approach away from the vertical axis. Therefore, after measuring this angle in the field, a coordinate transformation algorithm is developed to rotate the coordinate system to offset the identified tilt angle.

Step 2: System coordinate transformation to integrate radars' trajectory data from different intersection approaches: a system coordinate transformation algorithm was developed to integrate trajectory data from all radars into a reference coordinate system. This step involves further coordinate rotation based on the intersecting angles of intersection approaches, as well as offsetting the coordinate origin to the origin of the reference coordinate system.

FIGURE *5* illustrates the result of coordinate transformation based on field data collected. After coordinate transformation, all three coordinate systems representing trajectory data from Southbound, Eastbound, and Westbound approaches are integrated into a reference system with origin *O*.

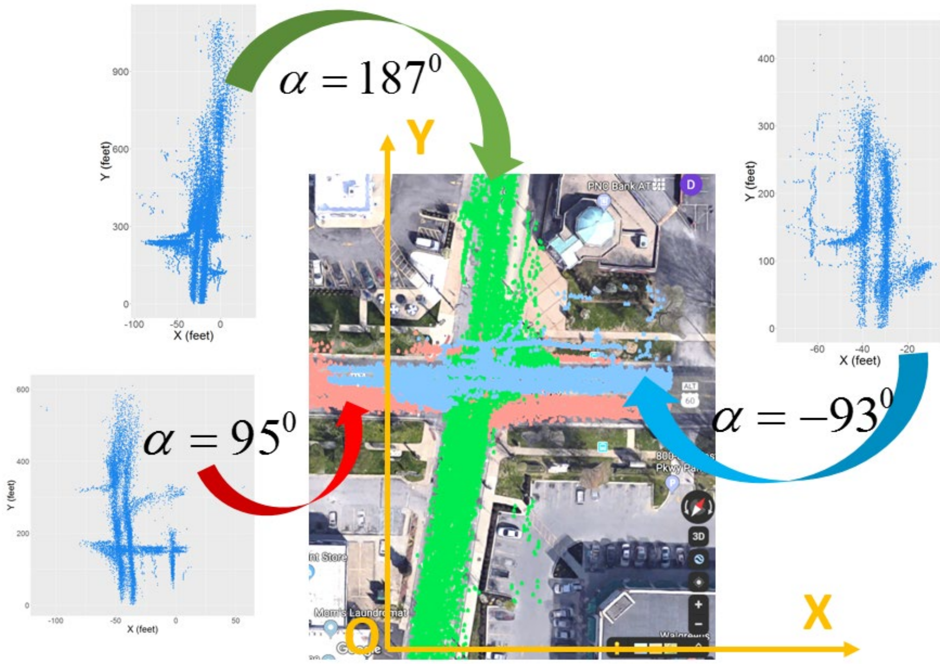

FIGURE 5 Coordinate transformation processing.

In the coordinate transformation process, the rotation angle and offset distance involved are based on measurements from Google Maps, which may cause errors. Therefore, a calibration process was developed to address the errors in the radar data integration process.

A calibration process was developed to correct the errors caused by coordinate transformation to ensure data accuracy after the data integration. In the calibration process, a drone that flies near the intersection to capture videos was used to record the intersection traffic from a bird's view. Ground truth coordinates of the target vehicle trajectories in the reference system were extracted from the drone video with the accurate measurement using Google Map's measurement tool. By matching the synchronized timestamps, the target vehicle in the video is then identified from the radar sensor data. The coordinate transformation algorithm is then calibrated by fine-tuning the rotation angle and offset distance by minimizing the error by comparing the target vehicle's coordinates after coordinate transformation to the ground truth coordinates of the same vehicle as measured from the video. **FIGURE *6*** illustrates the calibration process.

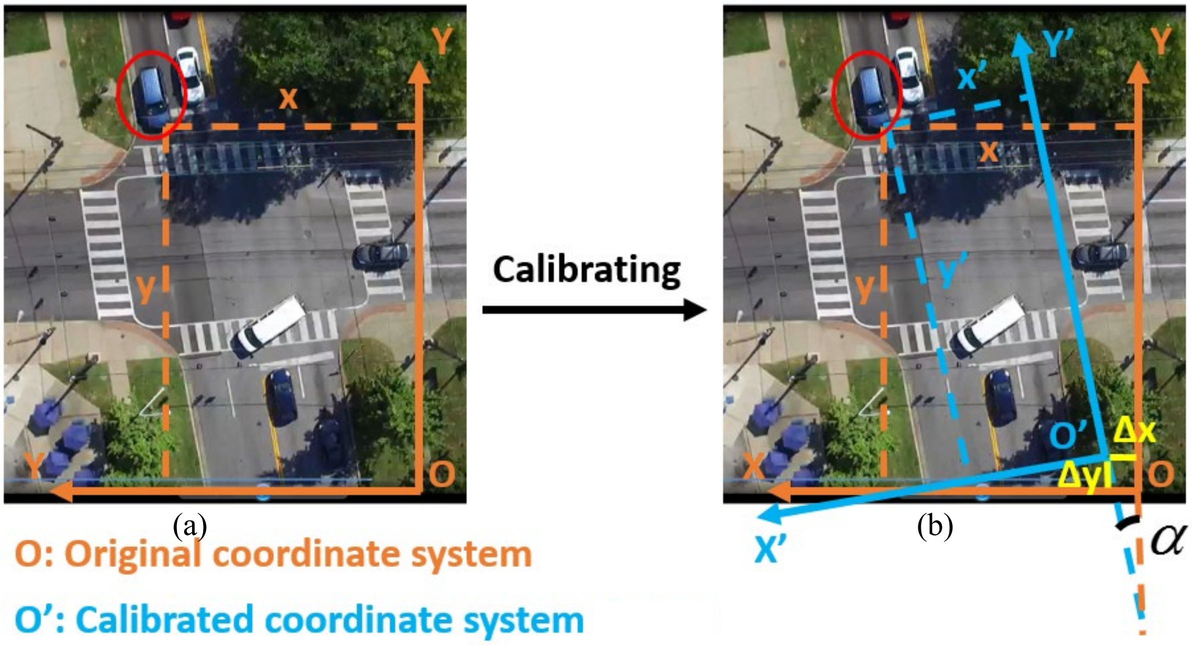

FIGURE 6 Calibration process in the radar data integration process: (a) uncalibrated coordinate system; (b) calibrated coordinate system.

Table 1 summarizes the test calibration result after using 10 vehicles in the drone video for each approach to calibrate the coordinate transformation algorithm.

TABLE 1 Result of the coordinate transformation algorithm calibration.

	Average X error (ft)	Average Y error (ft)
West Radar	-0.08	0.72
East Radar	1.57	1.16
North Radar	1.37	0.44

3.2.2 Development of Time-to-collision and Traffic Conflicts Computation

3.2.2.1 Time-to-collision (TTC) Calculation Module

An algorithm that calculates TTC for all possible conflicting movements was developed based on the trajectory data for different movements identified/classified by the movement classification module.

A traffic conflict is defined as an observable situation in which two or more road users approach each other in space and time to such an extent that there is a risk of collision if their movements remained unchanged. Time to collision (TTC) is generally recognized as the most frequently used indicator to identify a conflict. In terms of conflict types, two main types were defined by *Surrogate Safety Assessment Methodology* (SSAM) report as a conflict point and a conflict line type. The conflict point type reflects right-angle, vehicle-pedestrian, sideswipe, and left-turn angle conflict types. The conflict line type reflects rear-end conflict type only. For a wide recognition of these terms, right-angle, vehicle-pedestrian, sideswipe, and left-turn angle conflict types are generalized as a 'crossing' conflict type and rear-end conflict type is still denoted as a 'rear-end' conflict type.

In general, TTC is calculated assuming velocity vectors of a leading and following vehicle are on the same line, which can cause an error without considering the offset between these two vectors. Therefore, the algorithm uses two TTC calculation methods that are formulated respectively to target the rear-end conflict type and the crossing conflict types.

3.2.2.1.1 TTC Calculation for Rear-end Conflict Type

First, for each pair of leading-following vehicles without offset between their velocity vectors, the TTC can be continuously estimated over time in the following form:

$$TTC_t = \frac{X_{L,t} - X_{F,t} - D_L}{V_{F,t} - V_{L,t}}; \quad \forall\, (V_{F,t} - V_{L,t}) > 0 \tag{1}$$

Where t denotes a time instant, L denotes the leading vehicle, F denotes the following vehicle, X denotes the vehicle position, V denotes the vehicle, speed, and D denotes the vehicle length.

Second, for each pair of the leading-following vehicles with the offset between their velocity vectors, the TTC can be continuously estimated in time in the following form:

$$TTC_t^{RE,o} = \frac{\sqrt{(X_{L,r,t} - X_{F,f,t})^2 + (Y_{L,r,t} - Y_{F,f,t})^2}}{V_{F,t}\cos(\theta_{F,t}) - V_{L,t}\cos(\theta_{L,t})} \tag{2}$$

Where RE denotes the rear-end conflict type, o denotes the offset term, r denotes the rear bumper of vehicles, f denotes the front bumper of vehicles, θ denotes the offset, X and Y denotes the position vertices in a two-dimension coordinate system, and other parameters are defined as the same as Equation (1). This TTC calculation method is illustrated in ***FIGURE 7***.

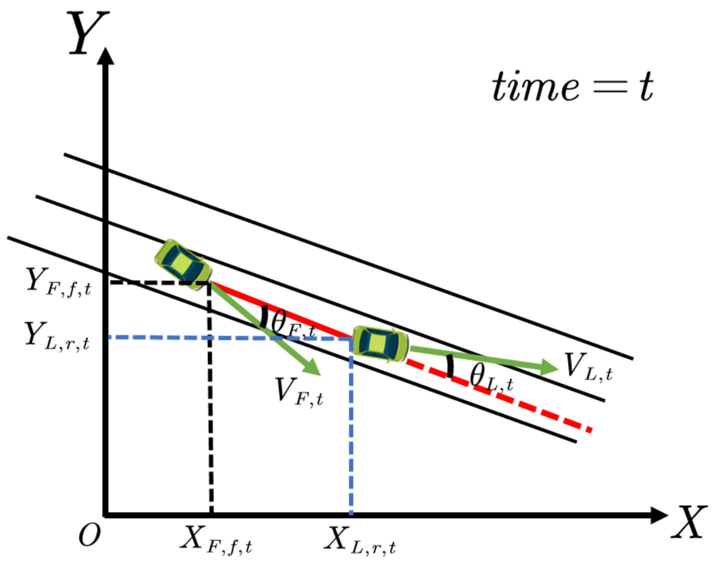

FIGURE 7 Rear-end TTC calculation with offset in a two-dimension coordinate system.

3.2.2.1.2 TTC Calculation for Crossing Conflict Types

For the crossing conflict indicator, different from Equations (1) and (2), it is formulated based on a two-dimension coordinate system because the offset exists as long as the velocity vectors of conflicting vehicles are not on the same line. The indicator is derived in the following form:

$$TTC_t^{Cr,o} = \frac{\sqrt{(X_{1,f,t} - X_{2,f,t})^2 + (Y_{1,f,t} - Y_{2,f,t})^2}}{V_{1,t}\cos(\theta_{1,t}) + V_{2,t}\cos(\theta_{2,t})} \tag{3}$$

Where in the denominator, the relative speed is a sum of velocity vectors of conflicting vehicles. The TTC indicator calculation method for the crossing conflict type is illustrated in ***FIGURE 8***.

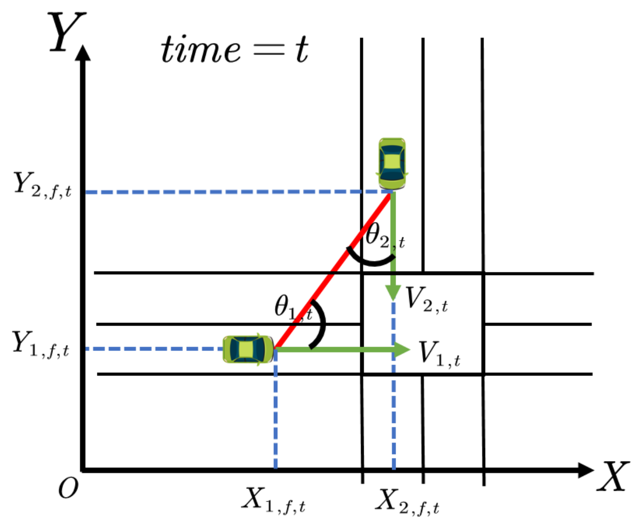

FIGURE 8 Crossing TTC calculation with offset in a two-dimension coordinate system.

3.2.2.2 Traffic Conflicts Identification Module

An algorithm was developed to identify traffic conflicts based on the TTC data calculated and create an output file of all identified traffic conflicts by conflict types, i.e., rear-end conflict type, and crossing conflict type. The output file includes coordinates of all conflicts identified, which will be used to display all the traffic conflicts on the intersection map. The output file also includes each conflict's type and severity as represented by TTC. Types of conflicts that are of concern in this algorithm are illustrated in ***FIGURE 9***. ***FIGURE 9*** (a) illustrates the rear-end conflict type, while ***FIGURE 9*** (b) to (f) represent different crossing conflict types.

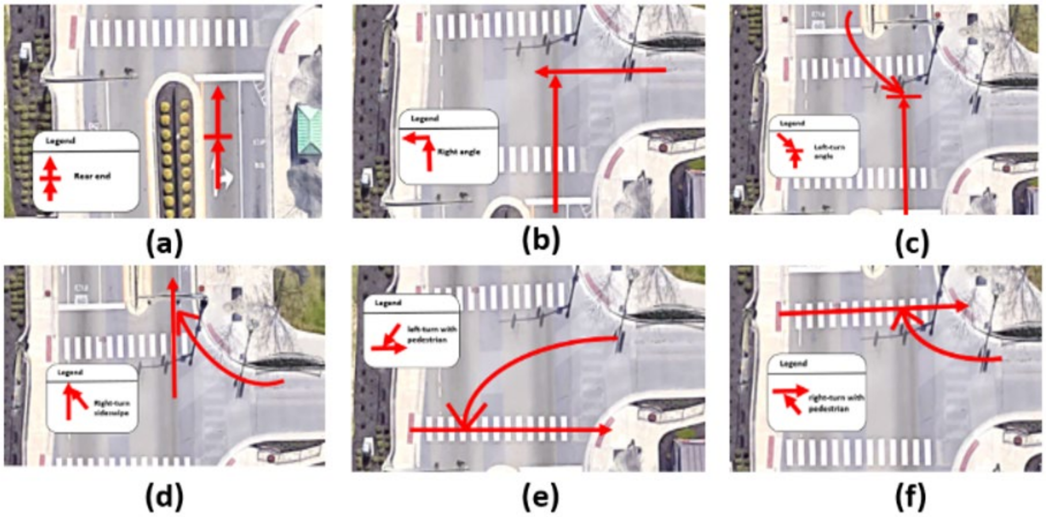

FIGURE 9 Types of traffic conflicts of concern: (a) rear-end conflict; (b) right-angle conflict; (c) left-turn angle conflict; (d) sideswipe conflict; (e) left-turn vehicle with pedestrian conflict; and (f) right-turn vehicle with pedestrian conflict.

Based on these specific conflict types of concern, TTC can be calculated for every conflicting trajectory data pair at every conflicting point, and a minimum TTC value of this event can be identified as the measurement for the severity of the conflicting trajectory data pair. Whether the severity qualifies for a traffic conflict is determined by the minimum TTC threshold to define a traffic conflict. This threshold is usually different for rear-end type conflicts and crossing type conflicts and is configurable in IPSV.

3.2.2.2.1 Minimum TTC Threshold for the Rear-end Conflict Type

For the rear-end conflict type, the TTC threshold of 1.5 s is commonly used by researchers to define conflicts (*21*). To determine the TTC thresholds ranging from 1 to 3 s explicitly, using an interval of 0.5 s provides a better understanding of different levels of risks (*22, 23*). Therefore, a threshold of 1.5 s is tentatively selected as the minimum TTC threshold to define a rear-end traffic conflict, however, this parameter was still kept configurable in the algorithm.

3.2.2.2.2 Minimum TTC Threshold for Crossing Conflict Types

For crossing conflict types, there is still a lack of a specific, common TTC threshold. Hirst and Graham (*24*) reported that a TTC of 4 s could be used to distinguish between higher risk and lower risk situations. In a driving simulator experiment, Hogema and Janssen (*25*) indicated that the critical TTC threshold is 3.5 s and 2.6 s for non-supported and supported drivers, respectively. The minimum TTC threshold for a crossing conflict type is assumed as a higher value than that of a rear-end conflict type in terms of a longer distance headway between conflicting vehicles (*26*). Therefore, to be on the safe side, a minimum TTC threshold of 4 s was tentatively used to determine crossing conflict types, however, this parameter was still kept configurable in the algorithm.

3.2.3 Proof-of-Concept Field Study

A field study at two closely spaced urban intersections in Louisville has been performed to evaluate the safety performance of these two intersections for the Kentucky Transportation Cabinet, and at the same time to prove the concept of IPSV. The radar trajectory data collection was conducted from July 10th, 2019 to July 16th, 2019 at Eastern Parkway @ S Preston St, and from July 24th, 2019 to July 30th, 2019 at Eastern Parkway @ S Shelby St. ***FIGURE 10*** illustrates the study sites.

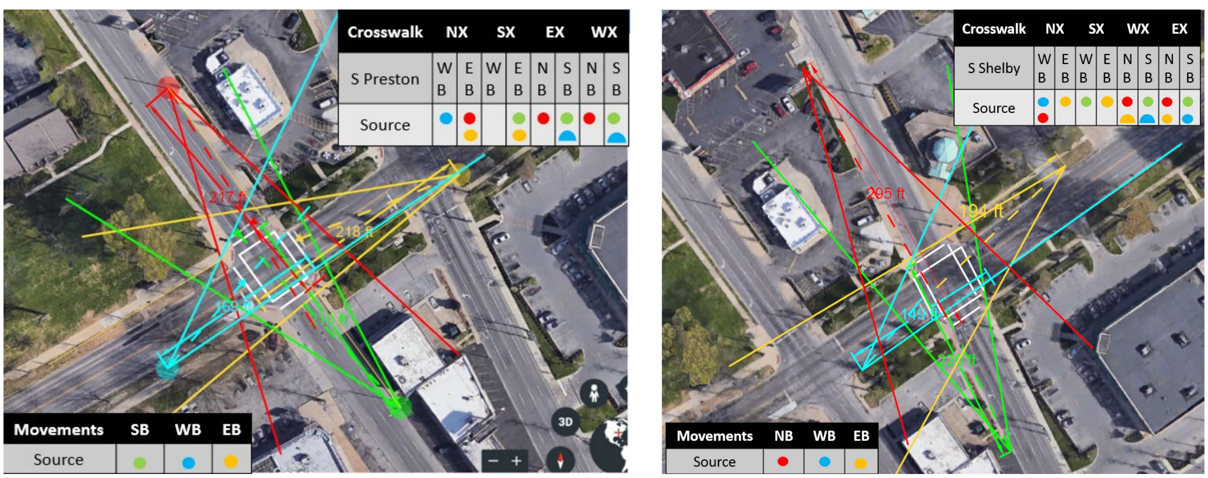

(a) (b)

FIGURE 10 Study site and radar setup: (a) Eastern Parkway @ S Preston St data collection; (b) Eastern Parkway @ S Shelby St geometry.

The IPSV algorithm was applied to the collected data. Due to the report length requirement, this section briefly summarizes the result for the Eastern Parkway @ S Shelby St Intersection only.

3.2.3.1 Movement Trajectories Classification

After data was preprocessed, trajectories of all traffic and pedestrian movements were identified and classified. ***FIGURE 11*** illustrates the trajectories for various movements at the intersection.

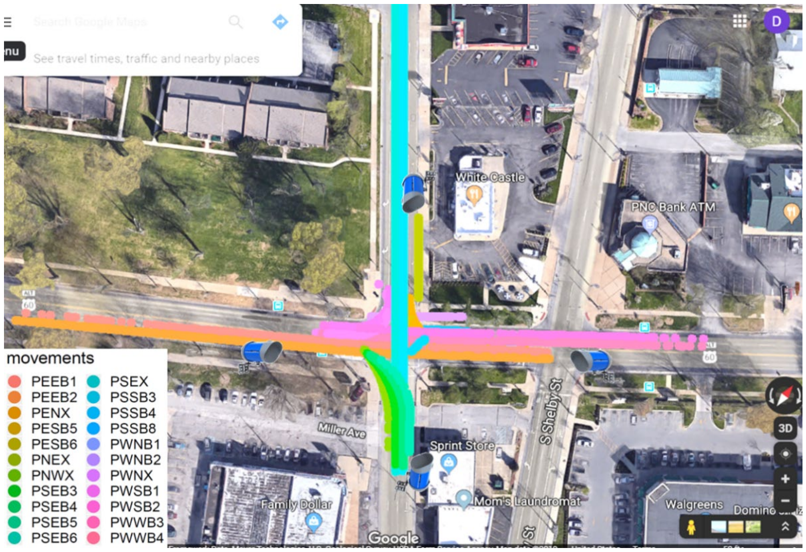

FIGURE 11 Classification of trajectories of various movements at Eastern Parkway @ S Preston St.

3.2.3.2 Traffic Conflict Detection Method

Traffic conflicts considered in this study include crossing conflicts and rear-end conflicts. Crossing conflicts consist of the following four types:

- Right-turn conflicts, as illustrated by black squares in ***FIGURE 12*** (a).
- Right-angle conflicts, as illustrated by black moon shapes in ***FIGURE 12*** (b).
- Left-turn conflicts, as illustrated by black triangles in ***FIGURE 12*** (c).
- Pedestrian-vehicle conflicts, as illustrated by the black lightning shapes in ***FIGURE 12*** (a).

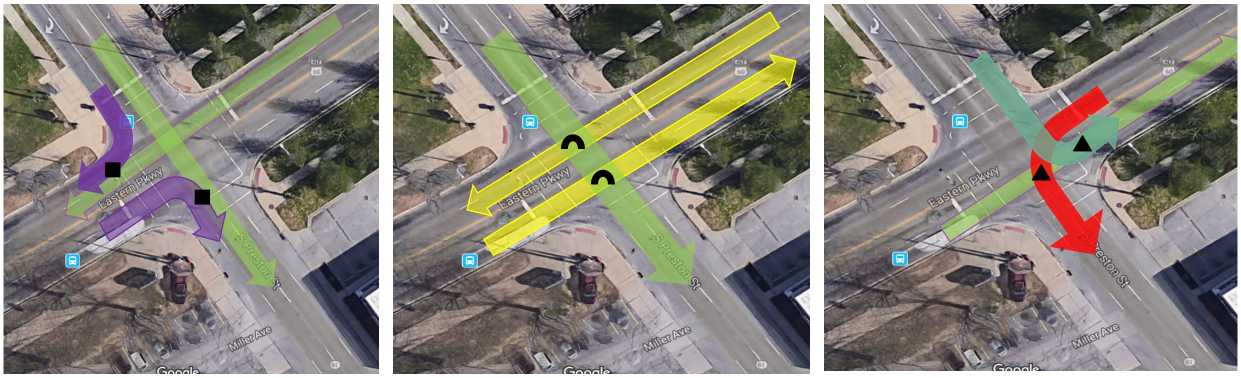

(a) (b) (c)

FIGURE 12 Crossing conflict types: (a) right turn conflicts; (b) right angle conflicts; (c) left turn conflicts.

Rear-end conflicts were detected for every movement from each approach. Movements, where rear-end conflicts were considered, are represented by black circles in ***FIGURE 13*** (b).

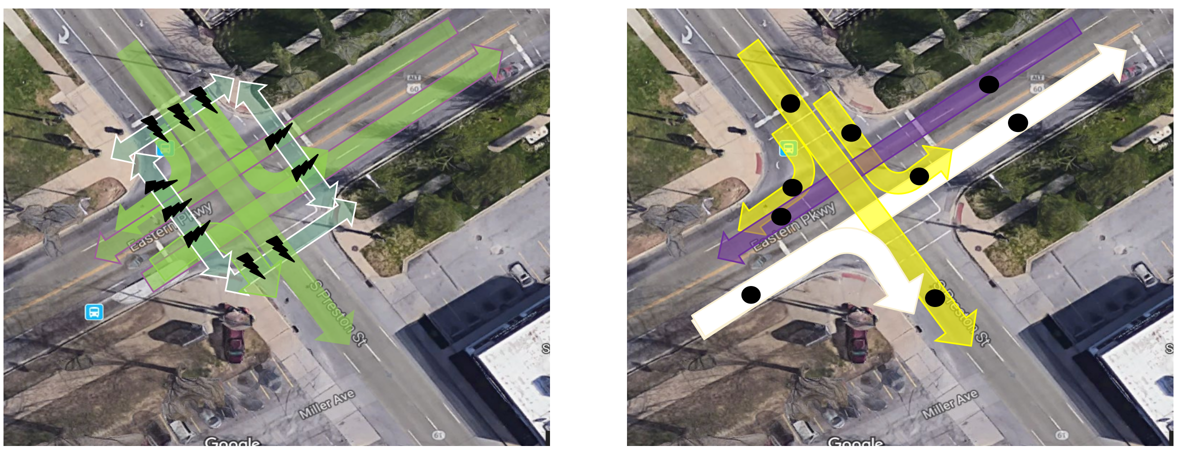

(a) (b)

FIGURE 13 Pedestrian and rear-end conflict types: (a) pedestrian-vehicle conflicts; (b) rear-end conflicts.

Time-to-collision (TTC) was used as a measure to define traffic conflicts. For rear-end conflicts, the TTC threshold is 1.5 s. For any crossing conflicts, Ozbay et al. (*27*) suggested a TTC threshold of 4 s. Therefore, 4 s was selected as the threshold to define a crossing conflict and 1.5 s was used as the threshold to define a rear-end conflict in this study.

3.2.3.3 Conflict Identification and Severity Analysis

Traffic conflicts including both crossing types and rear-end types were identified based on the TTC calculated. The severity of a traffic conflict is represented by the conflict's TTC. A lower TTC means a more severe conflict. All identified traffic conflicts are plotted on aerial maps, which are color-coded by TTC. More severe conflicts (lower TTC) are represented by red color.

3.2.3.3.1 Crossing conflict severity

All crossing conflicts with TTC under 4 s were extracted based on their minimum TTC value. Accordingly, conflict locations and conflicting vehicles' speeds were also extracted. The severity map for all crossing conflicts is illustrated in ***FIGURE 14*** (a). Conflicts within the northeast corner of the intersection are of higher severity.

3.2.3.3.2 Rear-end conflict severity

All rear-end conflicts with TTC ≤ 1.5 s were extracted based on their minimum TTC value. Accordingly, conflict locations and conflicting vehicles' speeds were also extracted. The severity map for all rear-end conflicts is shown in ***FIGURE 14*** (b). Most of the rear-end conflicts are detected in the right lane of the eastbound Eastern parkway and the right through lane of the southbound S Preston St approach.

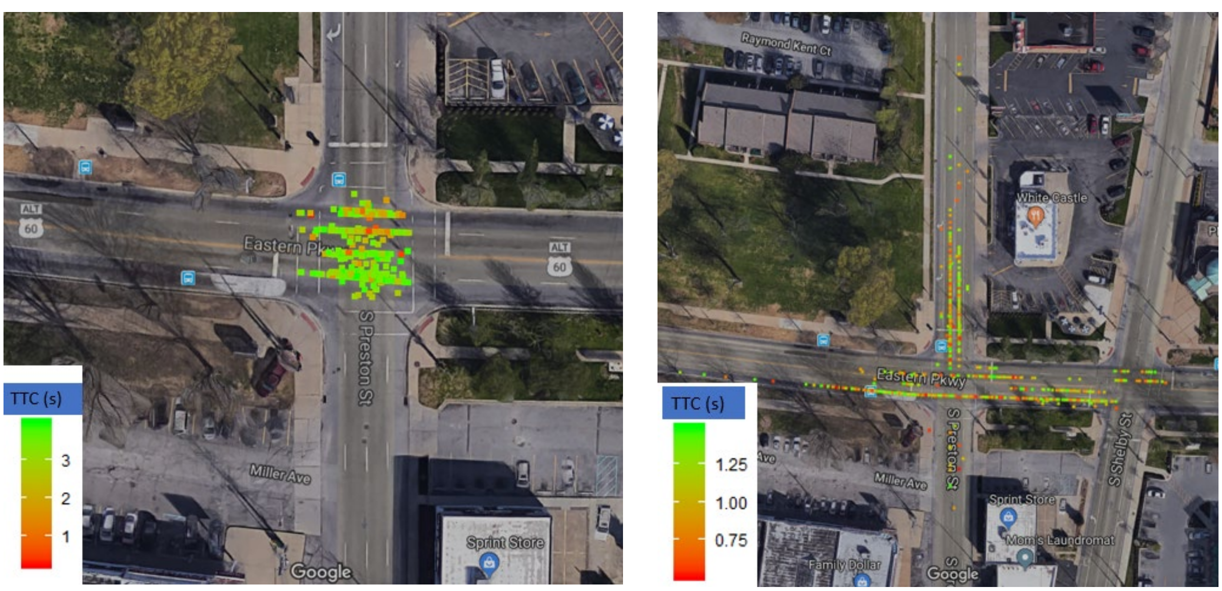

(a) (b)

FIGURE 14 Conflict severity by TTC: (a) crossing conflicts; and (b) rear-end conflicts.

3.2.3.4 Conflict Severity Determination by Speed

3.2.3.4.1 Crossing conflict severity

All crossing conflicts with TTC under 4 s were also analyzed by the speed at the minimum TTC. As shown in ***FIGURE 15*** (a). The speed of crossing conflicts between movements of eastbound approach and southbound approach is higher than those between movements of westbound approach and southbound approach.

(a) (b)

FIGURE 15 Conflict type severity by speed: (a) crossing conflicts; (b) rear-end conflicts.

3.2.3.4.2 Rear-end conflict severity

All rear-end conflicts with TTC under 1.5 s were analyzed by speed at the minimum TTC. As shown in ***FIGURE 15*** (b), most of the conflicts happened between a stopped vehicle and a moving vehicle. A severer conflict trend is detected in the right lane of the eastbound approach.

3.2.3.5 Crossing Conflicts by Conflicting Movements and Crossing Type

This section analyzes conflicts by conflicting movements and crossing types.

3.2.3.5.1 Crossing conflicts by conflicting movements

As shown in ***FIGURE 16*** (a), different crossing conflict groups by conflicting movements are illustrated by different shapes. Most of them are between SB through movements and EB through movements. One conflict between a vehicle and a pedestrian on the east side crosswalk and EB movements is also detected, as well as one conflict between WB illegal left turn and EB through movements.

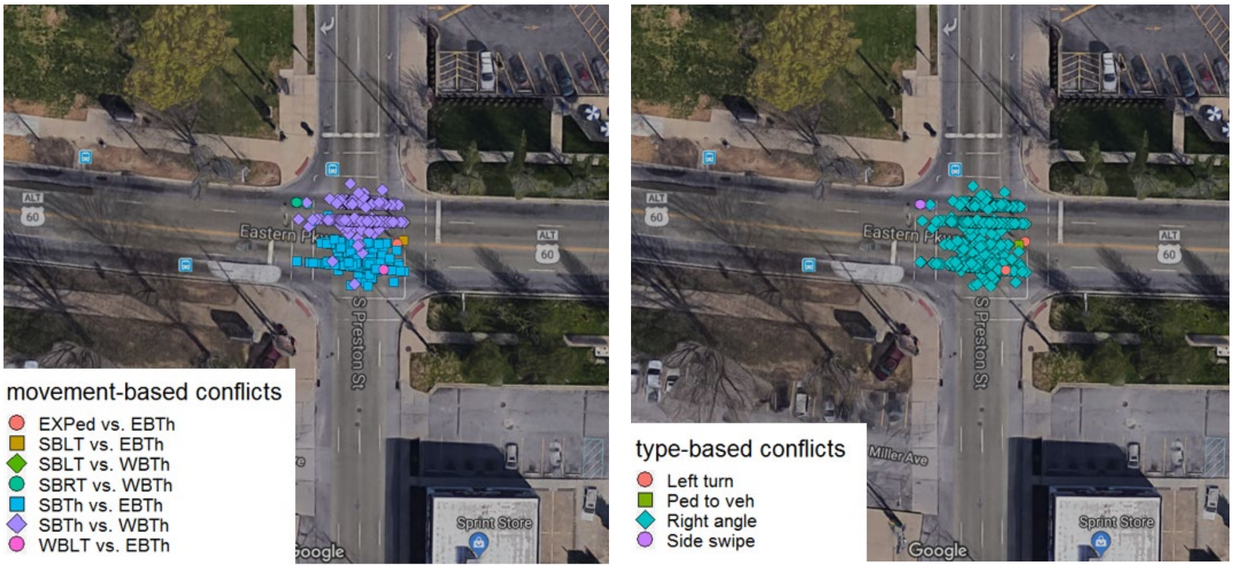

(a) (b)

FIGURE 16 Crossing conflict analysis: (a) by conflicting movements; (b) by crossing type.

3.2.3.5.2 Crossing conflicts by crossing type

As shown in ***FIGURE 16*** (b), four conflict types are illustrated by a different shape. Most of them are of right-angle conflict type. Some of them are left-turn angle, pedestrian-vehicle, or side-swipe conflicts.

3.2.3.6 Conflict Frequency Analysis

3.2.3.6.1 Crossing conflict frequency by weekday and time of day

As shown in ***FIGURE 17***, the frequency of crossing conflicts increases at peak hours and decreases at off-peak hours. Crossing conflicts are rarely detected before 5 AM. They mainly happen during work hours. Especially on Tuesday, an obvious upward trend is detected.

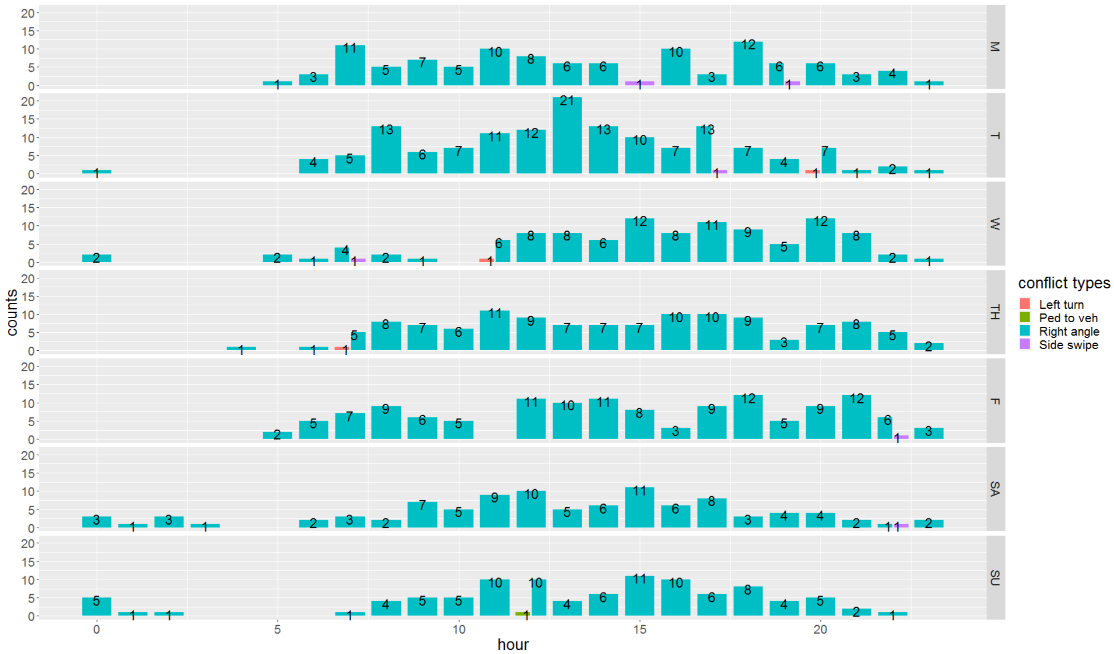

FIGURE 17 Crossing conflict frequency by the time of day and weekday.

In total, 823 crossing conflicts including all crossing types were detected during the week of data collection. ***FIGURE 18*** illustrates the distribution of crossing conflicts by crossing type and weekday. Weekends have lower conflict frequency compared to weekdays, possibly due to lower traffic volume.

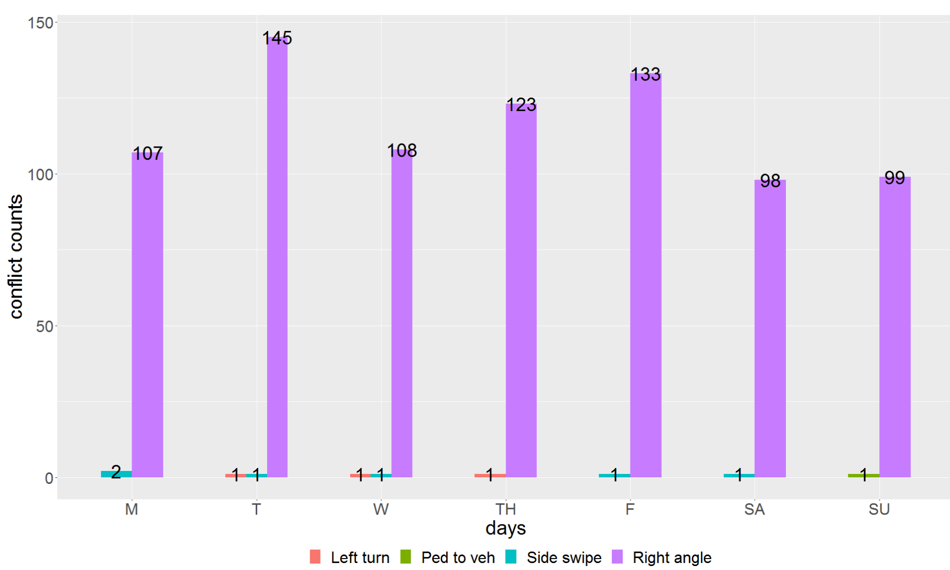

FIGURE 18 Crossing conflict frequency by type and weekday.

3.2.3.6.2 Rear-end conflict frequency by weekday and time of day

FIGURE 19 illustrates how rear-end conflicts are distributed in hours on different days of a week. As shown in ***FIGURE 19***, an obvious trend of increase before and decrease after peak hours is detected on weekdays. This trend is particularly reflected in the evening peak hours. Accordingly, rear-end conflicts are rarely detected before 5 AM.

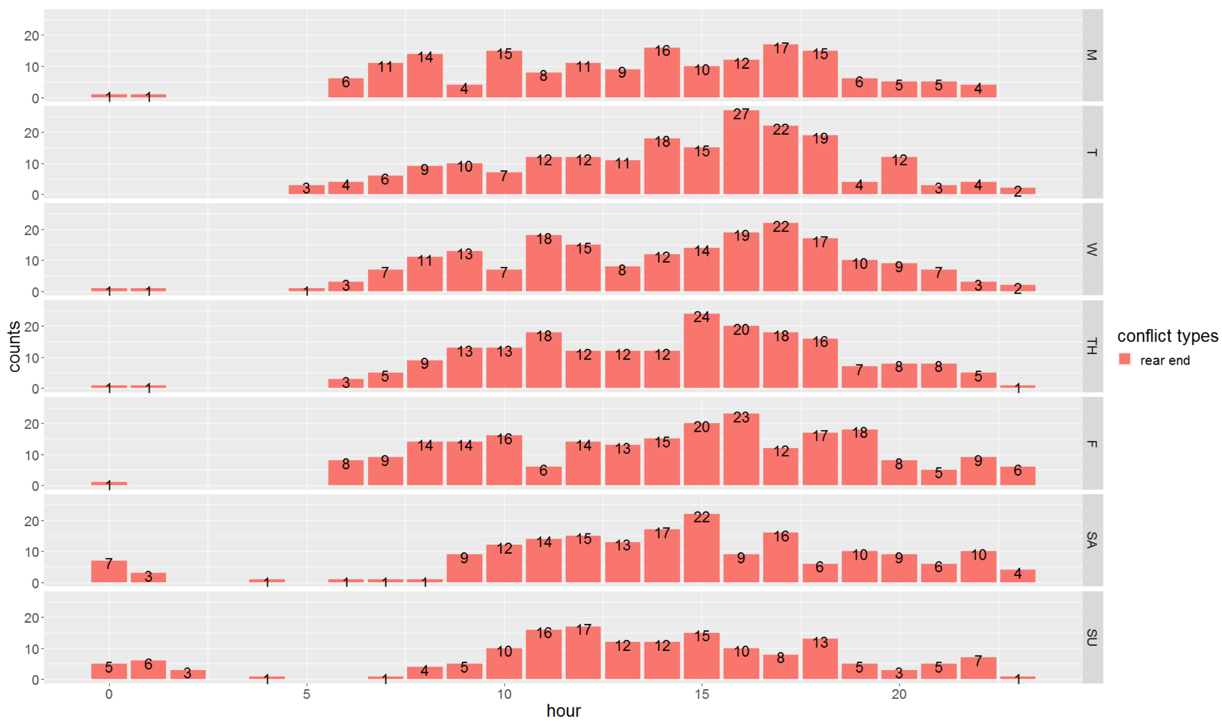

FIGURE 19 Rear-end conflict frequency by the time of day and weekday.

In total, 1,349 rear-end conflicts were detected during the week of data collection. ***FIGURE 20*** illustrates the distribution of rear-end conflicts by weekdays. Friday has the highest frequency while Monday and Sunday have the least frequency.

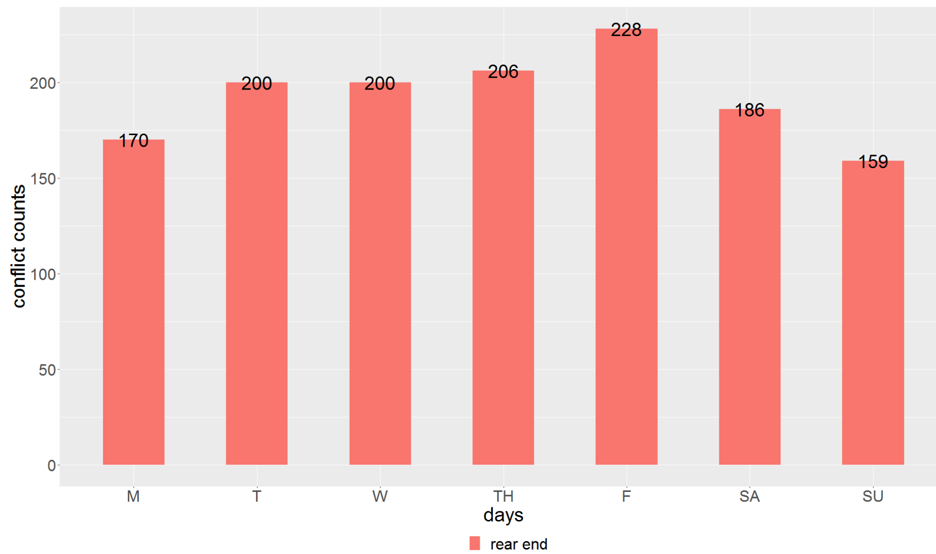

FIGURE 20 Rear-end conflict frequency by weekday.

3.2.3.7 Conflict Frequency by TTC Range

3.2.3.7.1 Crossing conflict frequency by TTC range

As shown in ***FIGURE 21***, crossing conflicts are mostly distributed in the TTC range between 1.5 s and 4 s. Crossing conflicts within the TTC range of 3.5 s to 4 s have the most frequency.

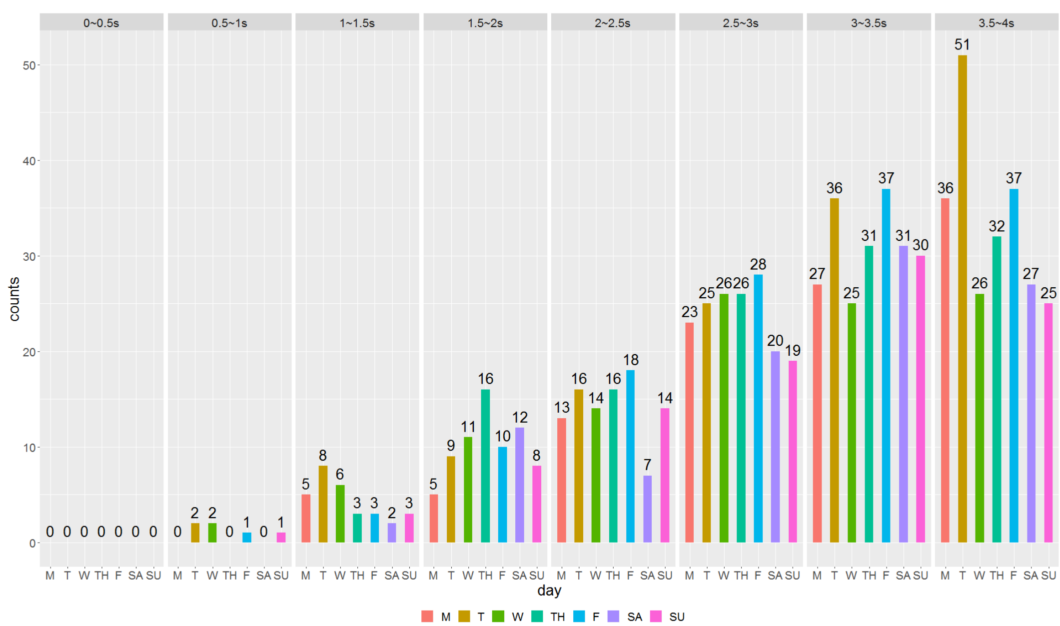

FIGURE 21 Crossing conflict frequency by TTC range.

3.2.3.7.2 Rear-end conflicts by TTC range

As shown in ***FIGURE 22***, no rear-end conflict was detected with TTC under 0.5 s. Rear-end conflicts are distributed the most on Thursday and Friday. The frequency of rear-end conflicts with TTC between 0.5 s and 1 s is less than that of conflicts with TTC between 1 s and 1.5 s.

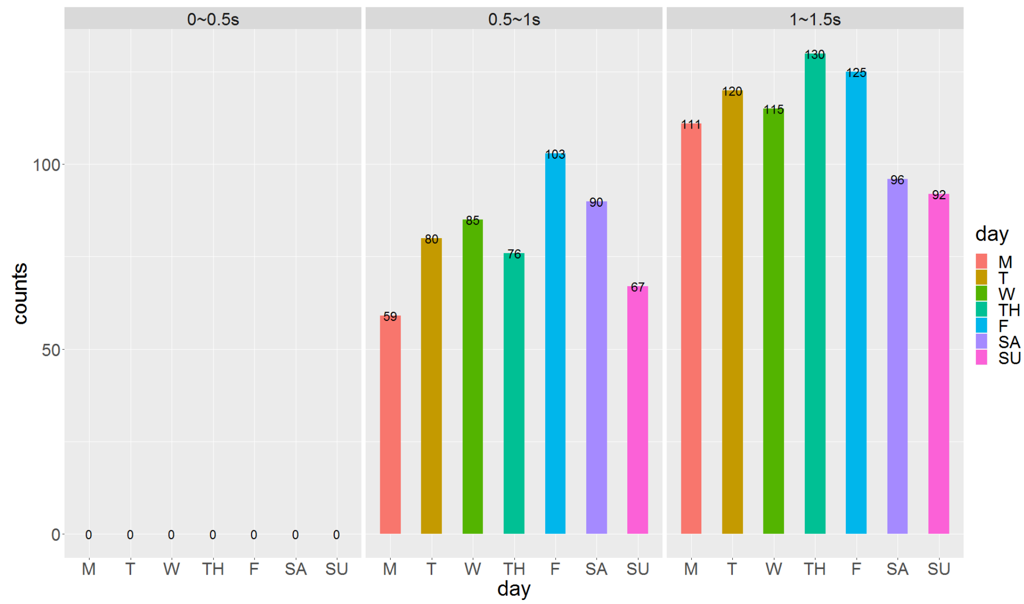

FIGURE 22 Rear-end conflict frequency by TTC range.

3.2.3.8 TTC Variance vs. Traffic Volume

3.2.3.8.1 Crossing TTC vs. traffic volume

As shown in ***FIGURE 23***, with traffic volume increasing at peak hours, especially evening peak hours, a decreasing TTC trend is detected during weekdays. The traffic volume of the southbound approach is higher than the other two approaches. The traffic volume of the westbound approach is the least. While volume keeps consistent at off-peak hours, the average TTC of crossing conflicts keeps relatively constant. However, there is high volatility of TTC on Saturday early morning with low traffic volume. Speeding issues could be the potential cause.

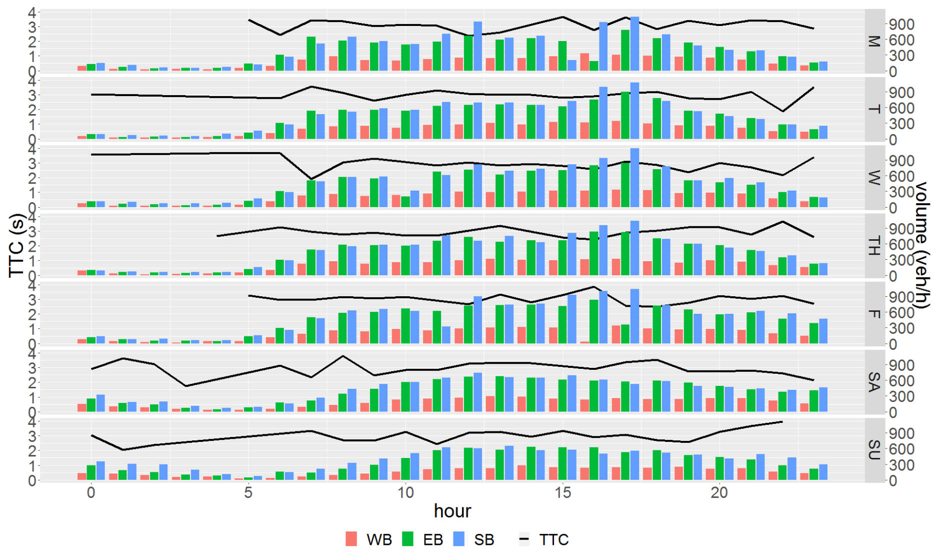

FIGURE 23 Crossing TTC variance vs. traffic volume.

3.2.3.8.2 Rear-end type TTC vs. traffic volume

As shown in ***FIGURE 24***, the average TTC of rear-end conflicts decreases during morning peak hours while the traffic volume increases rapidly.

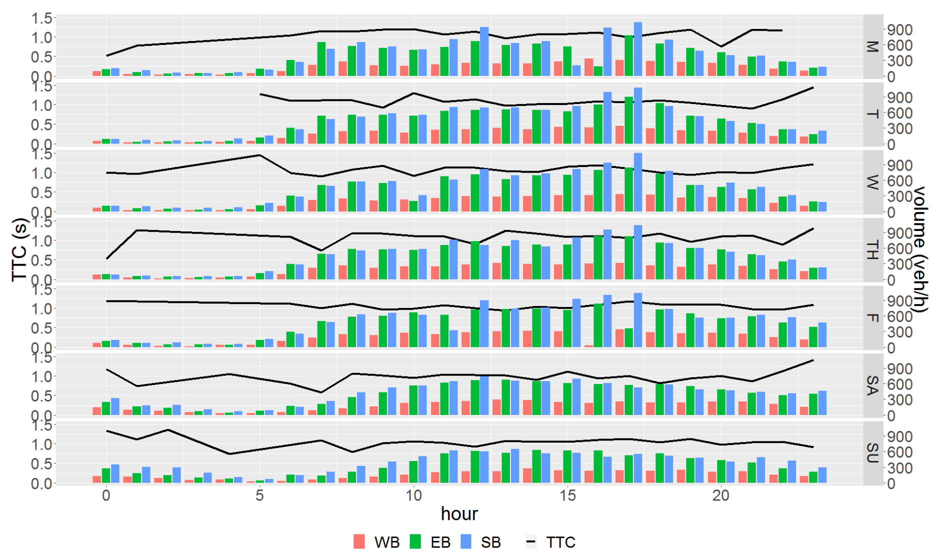

FIGURE 24 Rear-end TTC variance vs. traffic volume.

An obvious TTC decreasing trend is revealed during Monday evening peak hours. Similarly, high volatility of TTC is detected on Saturday early morning. Speeding issues could be the potential cause.

3.2.3.9 Traffic Events Analysis

3.2.3.9.1 Illegal left turns for westbound traffic

As shown in ***FIGURE 25***, illegal left turns are detected at different times of day, as westbound left turns are prohibited by the traffic sign. No illegal left turns were detected on Friday. Most illegal left turns happened on Tuesday afternoon. In addition, 5 cases in total were detected before 5 AM during the week of data collection.

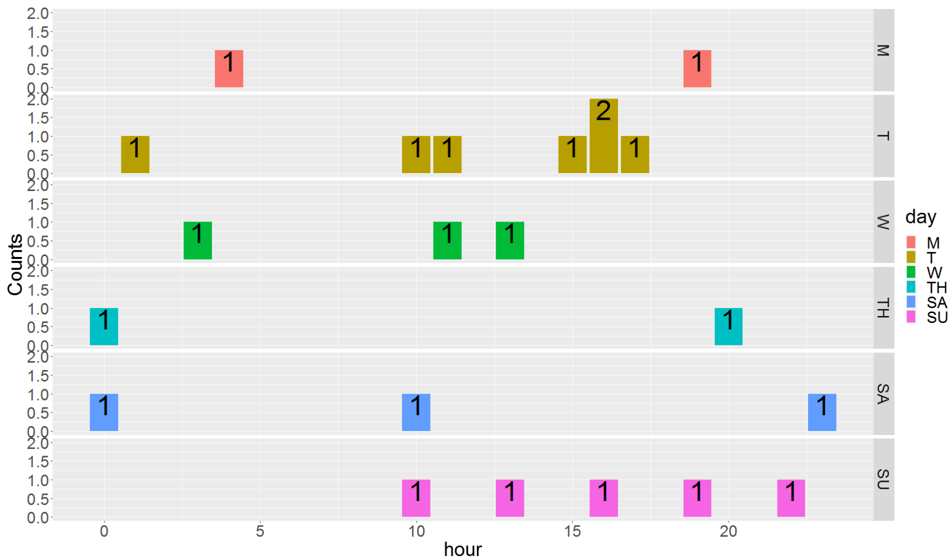

FIGURE 25 Illegal left turn counts.

3.2.3.9.2 Jaywalking Analysis

Jaywalking activities and counts were detected and summarized along with a comparison to counts of the pedestrian using the crosswalks. The 7-day jaywalking data was aggregated by hours to represent the pedestrian activities for the 24 hours within the week. ***FIGURE 26*** illustrates an example that shows the jaywalking activities during the hour between 5 AM and 6 AM of the whole week. The trajectories represented by white color indicate the jaywalkers.

	Jaywalkers	Pedestrians on crosswalk
Counts	5	14

FIGURE 26 Example of jaywalking activities.

3.3 CONCLUSIONS

The proof-of-concept field study has proven the prototype of IPSV and demonstrated its ability to capture vehicle-vehicle and vehicle-pedestrian traffic conflicts and their severity. In conclusion, ***FIGURE 27*** visualizes a summary of the tasks that have been completed in Stage 1. The IPSV algorithm has been developed, which includes intersection mapping, data integration from different radar data sources, data preprocessing, radar data calibration, movement classification for all approaches, computation of TTC for rear-end and crossing conflict events, and identification and visualization of traffic conflict results by location and severity.

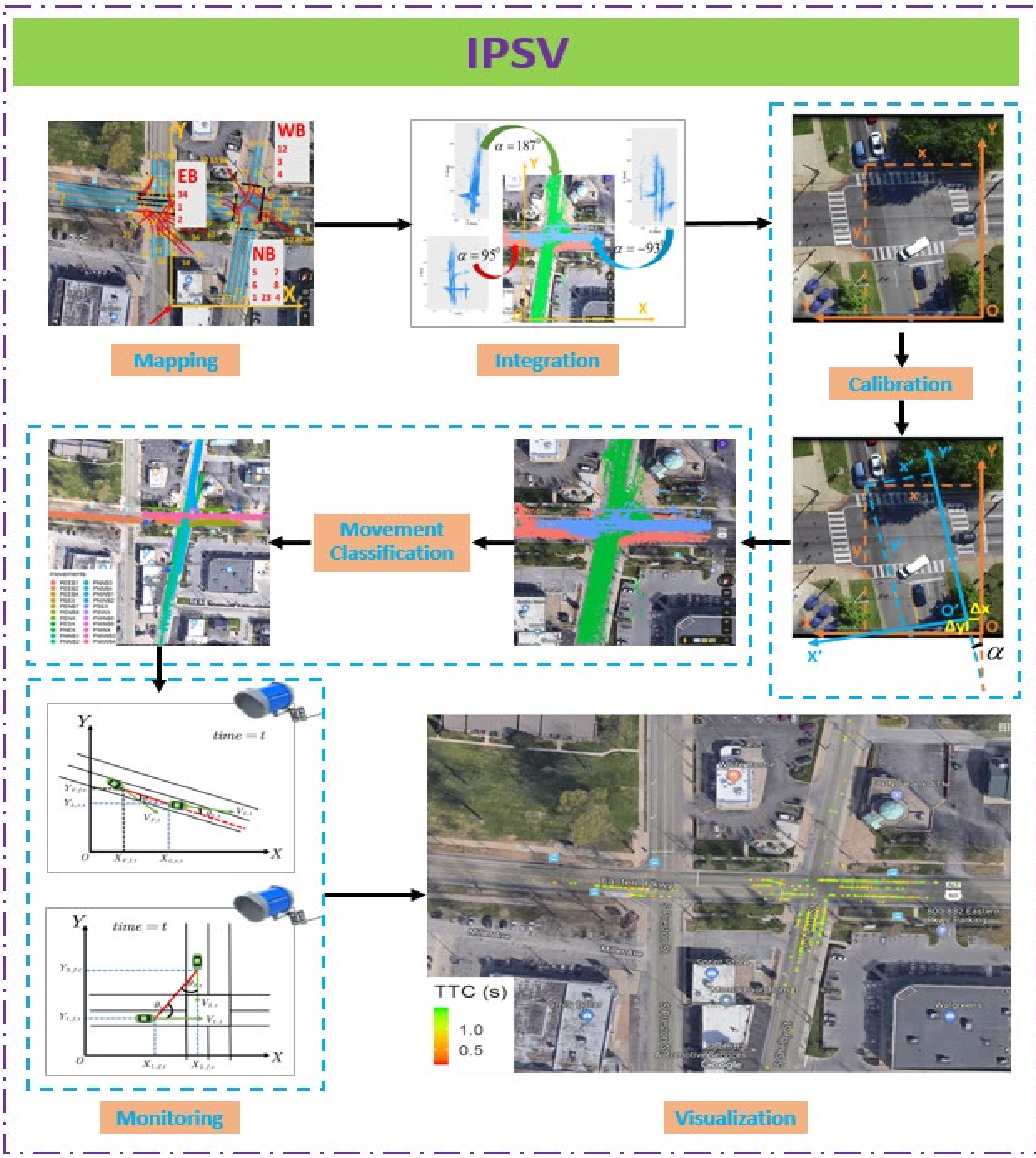

FIGURE 27 Stage 1 Tasks of IPSV Algorithm Development and Proof-of-Concept Field Study.

The next stage of work will focus on further addressing the issues identified in Stage 1, developing the configuration interface, achieving the real-time feature, finalizing the prototype, and testing and validating the IPSV.

4. IPSV DEVELOPMENT IN STAGE 2

4.1 IMPROVEMENTS IN IPSV ALGORITHMS

The algorithms in Stage 2 of the IPSV are updated from two aspects: fully automated application for any kind of intersection and more accurate conflict detection based on severity and quantity. The new characteristic of the IPSV, a more automated algorithm that can be applied to both unsignalized and signalized intersections, is realized by configuring lane/movement/stop bar values of any approach and measuring boundary values of an intersection from a satellite map. The other characteristic of the IPSV, more accurate conflict detection based on severity and quantity, is updated by distinguishing pedestrians/bicyclists from vehicles, smoothing trajectory based on in/extrapolated points, estimating the baseline of each lane, classifying trajectories by lanes, removing stopping trajectories, distinguishing rear-end/lane-change/left-turn angle/right-angle/sideswipe/pedestrian-to-vehicle conflicts based on conflict angle and introducing a new surrogate conflict index. The latter characteristic of the IPSV is also achieved in full automation.

4.1.1 Accurate Conflict Severity and Quantity Detection

4.1.1.1 Target Trajectory Retrieval for Each Radar

To distinguish trajectory points from conflicting approaches that are collected by a radar sensor that faces the other approach, a distance between the radar sensor and the stop bar of the oncoming approach is critically needed. Since the removal algorithm of this type of noise performed in Stage1 requires much time-demanding manual configuration in the IPSV, the method to remove this type of noise is updated in Stage 2. As shown in the FIGURE 28, the distance from the stop bar of the oncoming (target) approach to the radar sensor facing the approach is required to distinguish the conflicting trajectories from the other approach (shown in blue) from the target trajectories (shown in red). The conflicting trajectories will be removed, and the target trajectories will be kept to the most extent by this easy step. This target trajectory retrieval for each radar is also used in (*4*).

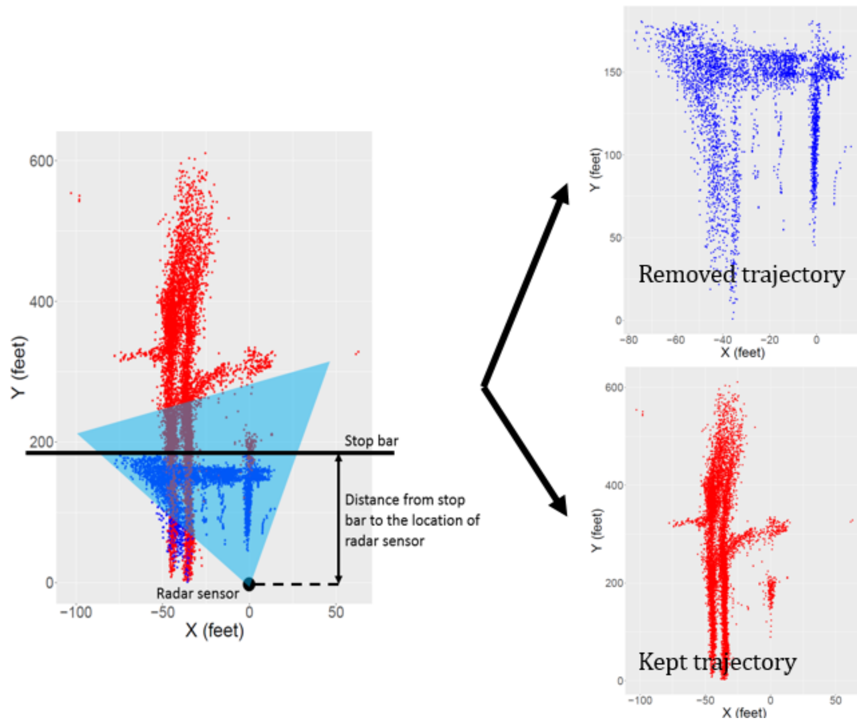

FIGURE 28 Target trajectory retrieval for each radar.

4.1.1.2 Correction of Trajectory Points by Longitudinal Displacement

Certain trajectory points of certain turning vehicles or vehicles moving with low speed, e.g., 2ft/s or 3 ft/s, sometimes will jump over their last trajectory point along the Y-axis in terms of the radar used for collecting the trajectories. In other words, the trajectory points will have longitudinal displacement error sometimes. This kind of problem happens during vehicles making a turn or move at a low speed because the radar is insensitive to moving objects in a direction perpendicular to the facing direction of the radar, and to the objects moving at a low speed.

The situation was observed in Stage 1 and the related points were directly deleted once they are identified by IPSV. In Stage 2, these kinds of points will not be deleted but estimated with new ones based on their adjacent last point to keep the quantity of the points and maintain the consistency of the points in terms of the longitudinal direction. After this step is updated in Stage 2, the quality of the trajectory points will be further improved.

The FIGURE 29 shows the trajectories with longitudinal displacement error from a test field database, where the identified errors are marked with red points. The figure also shows the before-and-after displacement error correction, where (a) describes the shape of errors when making a turn and (b) describes the estimated trajectory, in which all the errors are estimated based on their adjacent last trajectory point by assigning the same longitudinal coordinate of their last one to the following one in terms of time.

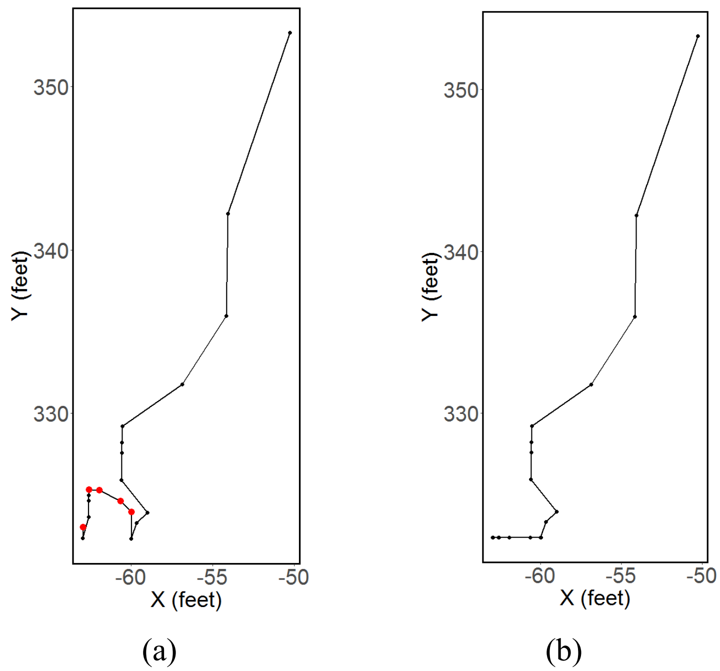

FIGURE 29 Correction of trajectory points by longitudinal displacement.

4.1.1.3 Trajectory Smoothing and Extrapolation

Positioning errors of tracking objects by radars may be caused by the radar itself shaking by winds. This kind of error is inevitable for any kind of sensor for object tracking on the road. This type of error was identified in trajectories and the whole trajectory was snapping onto a baseline of a lane, where the trajectory belongs, in Stage 1. This snapping method could eliminate the errors of each trajectory, however, could also eliminate lane-changing maneuvers if the trajectory is a lane change. In addition, vehicles may not exactly move along with the baseline of a lane in reality; regarding this situation, new errors may be introduced into the trajectories after snapping. Therefore, the snapping method is removed from Stage 2 and replaced by the smoothing method for each trajectory individually. As shown in the FIGURE 30, the bearing angle of each trajectory point is first calculated. Those points with a bearing angle more than the 85th percentile value of all bearing angles of the individual trajectory will be ‘virtually’ removed from the black line in **FIGURE *30*** (a) to the red line in **FIGURE *30*** (b).

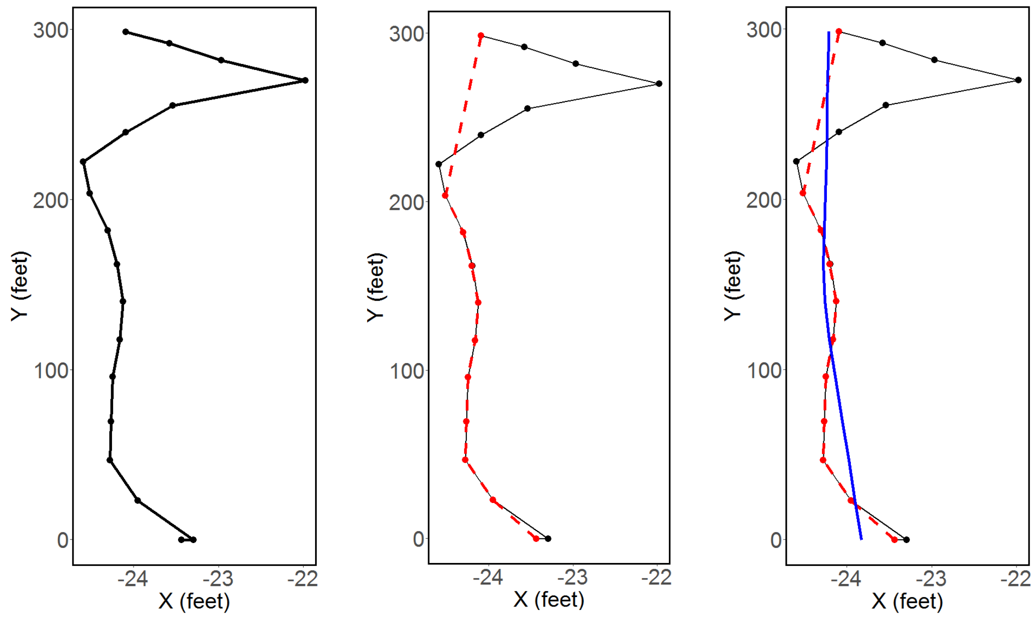

(a) (b) (c)

FIGURE 30 Trajectory smoothing.

The bearing angle is calculated as shown in the following FIGURE 31.

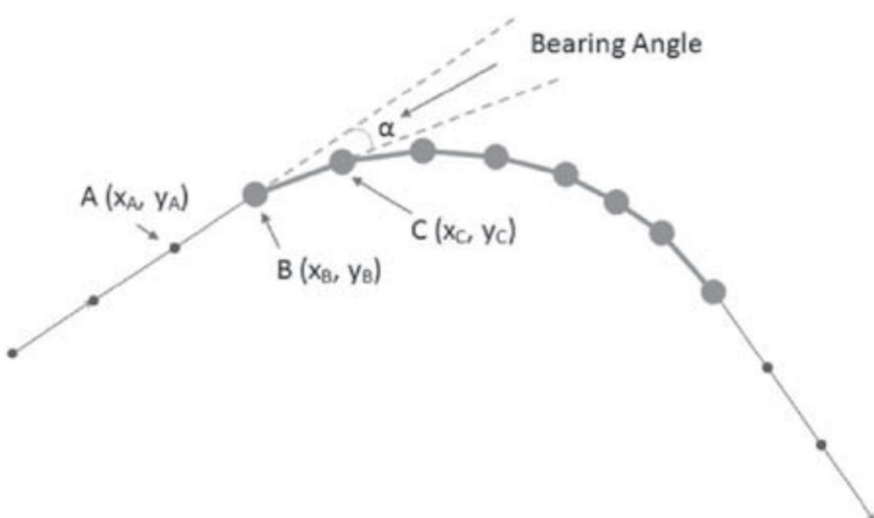

FIGURE 31 Bearing angle calculation (*28*).

After the virtual removal of each trajectory, the new trajectory will be extrapolated by the remaining points and those removed points will be extrapolated on the new trajectory. Such as in

FIGURE ***30*** (c) and **FIGURE** ***32*** (c), the blue trajectory is the extrapolated trajectory of the original black trajectory. The smoothing method is applied based on local polynomial regression fitting (Loess) (*29, 30*).

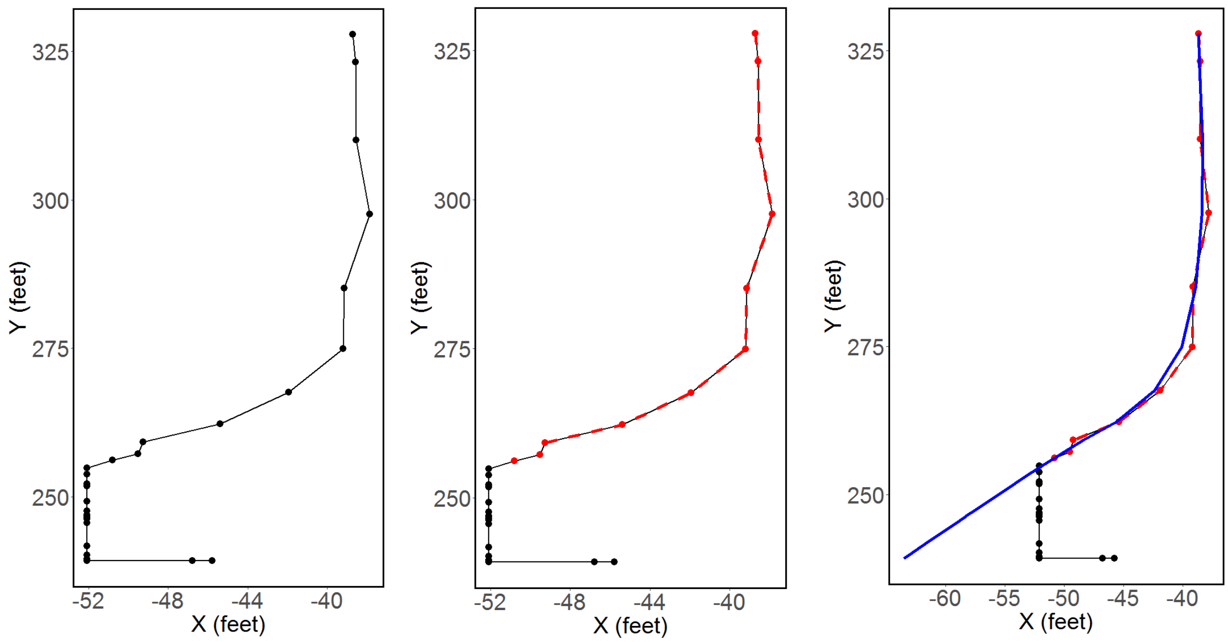

(a) (b) (c)

FIGURE 32 Trajectory smoothing and extrapolation.

4.1.1.4 Trajectory Data Time Synchronization

The 24GHz microwave doppler radar sensor has a 10^2 millisecond time precision. The time format of each trajectory point is recorded as 10.49 s or 10.52 s. The value in milliseconds differs for each vehicle and each radar sensor. When calculating conflicts, the value in milliseconds should be synchronized in the same format, e.g., 0 or 500 milliseconds. Each trajectory point is projected for its position from its original data time to a new data time based on the new format. As shown in FIGURE 33, the blue trajectory with red points is the new projected polyline from its old trajectory on the right. The time synchronization of each point is based on its proximity to the new format, e.g., 10.49 s is synchronized to 10.50 s and 10.8 s is synchronized to 11 s. Therefore, the conflict can be calculated across different radar sensors in a synchronized time. The synchronization is further made automated in Stage 2.

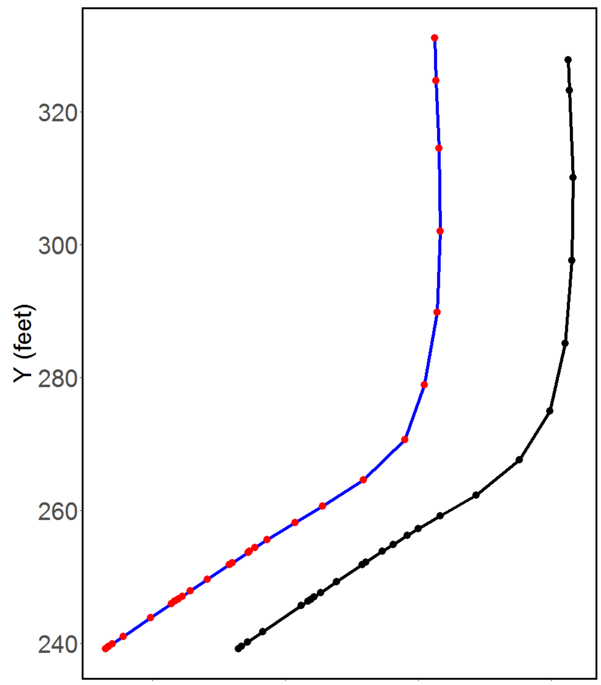

FIGURE 33 Trajectory point data time synchronization.

4.1.1.5 Estimation of Center Baseline of Each Lane

The center baseline of each lane of an approach is critical information for automated movement classification, lane changing detection, and further, conflict type classification. The baseline was manually measured from a Google satellite map in Stage 1. However, this step was time-demanding and manual errors would be introduced into the classification steps. In Stage 2, *this baseline estimation step is made automated and able to apply to any type/number/geometry shape of lanes of an approach*.

First, trajectories that are coming from upstream at top of the stop bar of the oncoming approach and moving downstream from the stop bar of the opposite approach are retrieved from all trajectories collected by a radar. As shown in **FIGURE** *34* (b), these trajectories are retrieved from four lanes at the upstream intersection.

Second, those retrieved trajectory points are clustered by a given number of center(s) every 50-feet segment along the longitudinal direction. The given number of center(s) of an approach is a predetermined number based on the number of lane(s) crossing through the intersection upstream to downstream. The number of lane(s) is called number of center lane(s).

As shown in **FIGURE** ***34*** (a), the number of centers is 2 in this case. The clustering method is based on K-Means clustering (*31*).

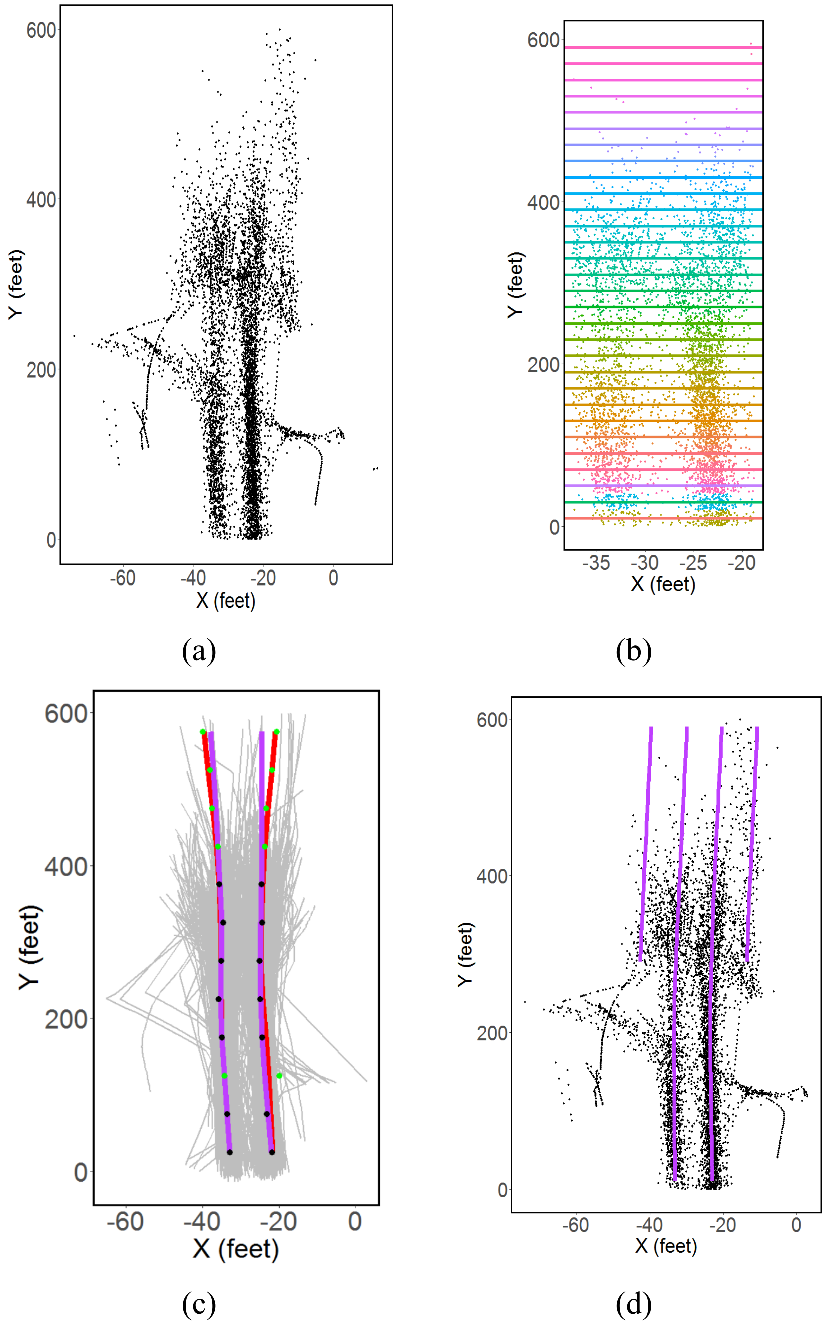

FIGURE 34 Methodology of center baseline estimation.

Third, a standard deviation of trajectory points at each 50-feet segment of the center lane(s) is calculated. Those cluster centers in certain segments are removed for further estimation if their standard deviation values are larger than the 90^{th} percentile value of all standard deviation values of all the segments. As shown in **FIGURE** ***34*** (c), these removed segment centers are marked as green points. This step could eliminate statistically insignificant centers if trajectory points at these segments have larger deviations than others.

Fourth, the center baseline of each lane is further smoothed based on the statistically significant centers, as shown in black points in **FIGURE *34*** (c). The smoothing method is also based on Loess. Based on the new smoothed baseline(s), an average lane width can be estimated. Therefore, the center baseline(s) of any lane on the right or left side of the center lane(s) can be estimated based on the average lane width. As shown in **FIGURE *34*** (d), center baselines of left/right and center lanes are smoothed and estimated.

It should be noted that this estimation method is immune to data loss or significant deviation at the upstream intersection. In this case, as shown in **FIGURE *34*** (a), trajectory points at center lanes above 400 feet and left lanes above 300 feet are statistically insignificant for baseline estimation. In addition, it is noted that this estimation method is made automated by acquiring the basic lane information from Google Maps, including the number of center/right/left lanes.

4.1.1.6 Movement Classification and Lane Change Detection

Based on the estimated baselines, each trajectory can be assigned a movement based on a minimum average mean distance difference between each point and baselines. If the average mean distance difference is larger than half of the average lane width, the movement is assigned based on the last point of each trajectory in terms of time. Furthermore, lane change maneuvers can be detected based on a minimum distance between each point and baselines at each time stamp. The movement classification and lane change detection are made fully automated in Stage 2. Such classification results are shown in FIGURE 35, where every trajectory is assigned a specific lane/movement. Further note that every trajectory will not be assigned multiple times on different lanes/movements based on the algorithm illustrate above.

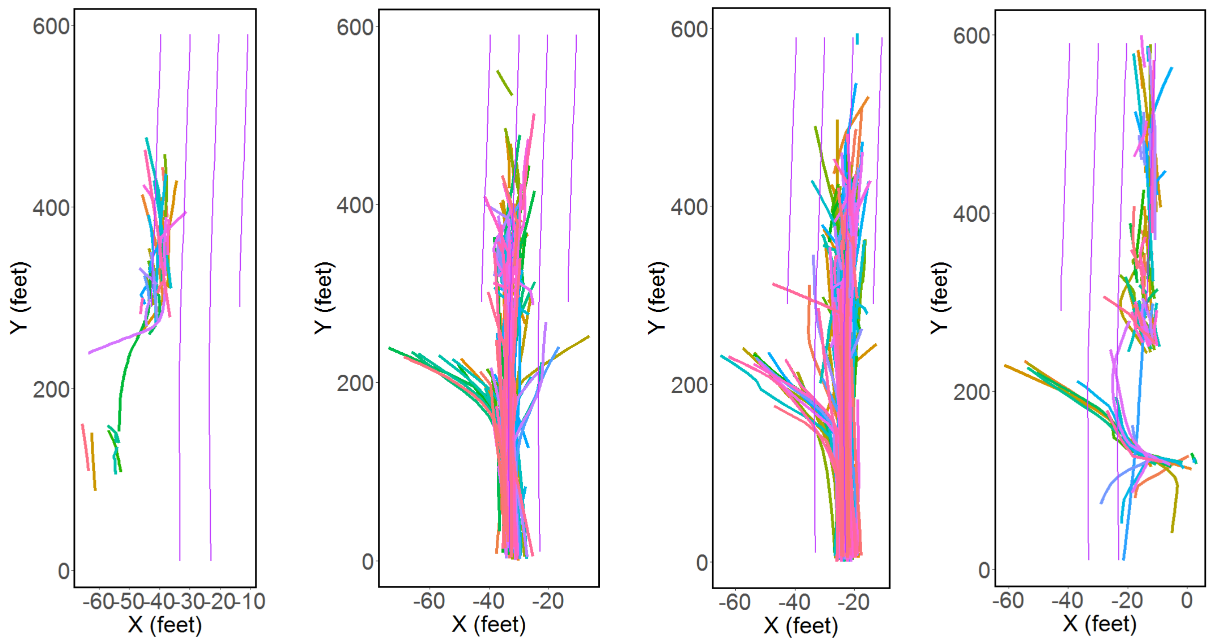

(a) (b) (c) (d)

FIGURE 35 Movement classification and lane change detection.

4.1.1.7 Removing Outlier/Stopping Trajectories

Some vehicles may stop in front of a stop bar for a period of time waiting for a green signal or waiting at a stop-controlled intersection. In such a case, the radar would lose tracking a vehicle and restart tracking this vehicle as a new vehicle if the vehicle stops for a long time and moves again. This problem could raise false positive conflicts when a following vehicle 'passes' the 'stopped' vehicle, and actually the following vehicle cannot pass its leader from the same lane. This problem was observed in Stage 1 and the number of false positive conflicts were not removed from conflict results in Stage 1. In Stage 2, such stopping trajectories are identified by a moving distance after a vehicle stops. Those trajectories that are first stopping and then moving again with the same vehicle ID are not removed. A threshold of the moving distance is the 85th percentile value of all such stopping trajectories. Those stopping points with a moving distance less than the threshold are removed. The FIGURE 36 shows the travel distances of vehicles from a sample dataset after the stopping points are removed. Given the empirical rule, more than 95% of the trajectories are retrieved for each dataset if the travel distance of a trajectory is larger than minus 2 standard deviations of the mean of all the distances. Given this step, statistical outliers are removed for each dataset. Those trajectories with a too short travel distance are not explainable.

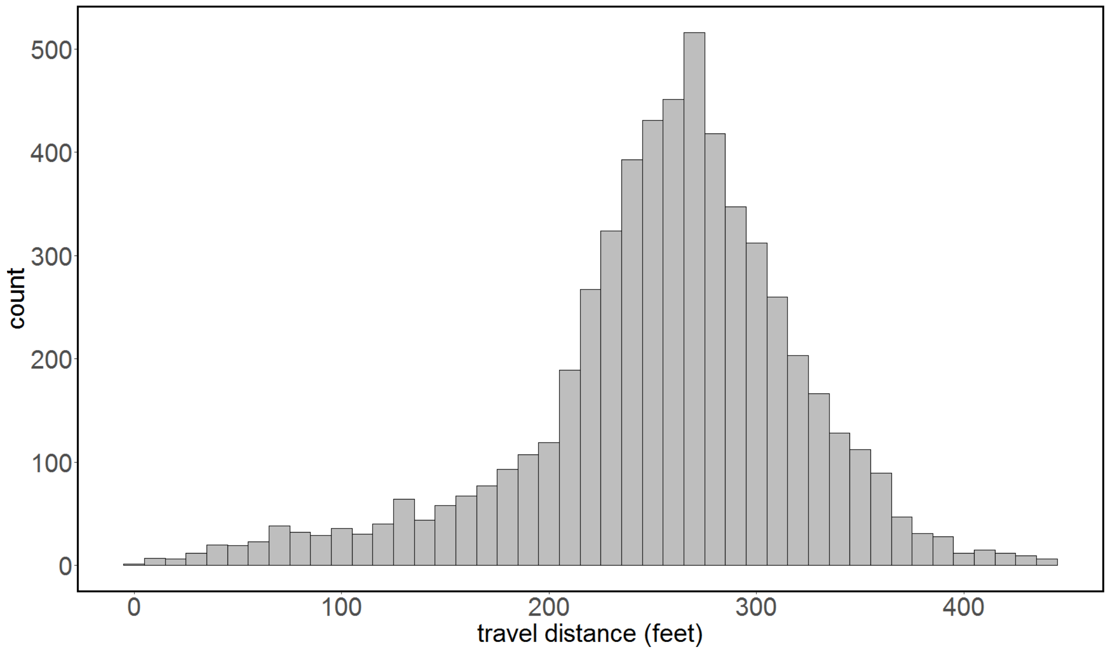

FIGURE 36 Histogram of travel distances.

4.1.1.8 Distinguishing Pedestrians/Bicyclists from Vehicles

Pedestrians/bicyclists (PBs) are marked by radar with a smaller object length than vehicles. However, some PBs may be recorded with an object length the same or larger than vehicles. In Stage 1, originally recorded object lengths, including vehicles' and PBs', are kept for TTC calculation during conflict events. To distinguish PBs from vehicles and improve the accuracy of TTC calculation, PBs are additionally marked in Stage 2 if their mean speed is less than 4 ft/s and maximum speed is less than 7 ft/s. PBs are thereby assigned a smaller object length than vehicles'. As shown in FIGURE 37, PBs are retrieved as red lines from a sample dataset, where blue lines are the same trajectories as left without smoothing.

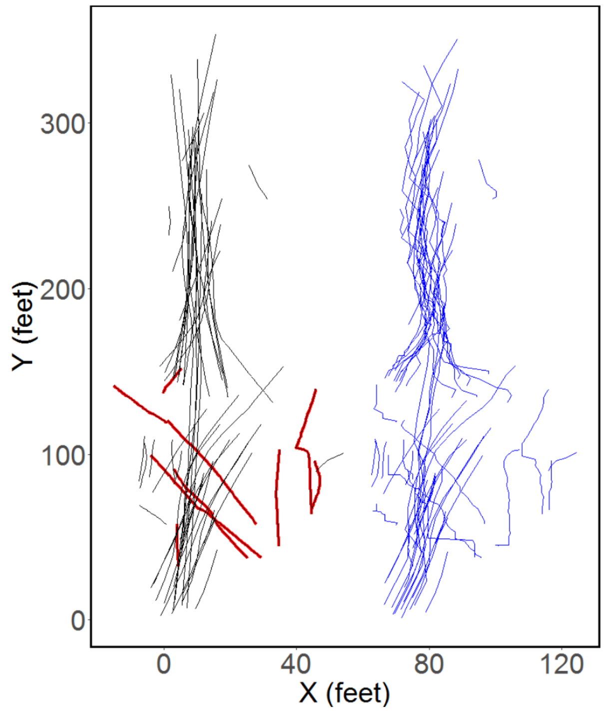

FIGURE 37 Distinguishing pedestrians/bicyclists from vehicles.

4.1.1.9 Estimation of Object Shape

The radar sensors only record the front (bumper) points of an object, including vehicles/PBs. The rear (bumper) points are also necessary for identifying the start and end of conflict events of any conflicts other than rear-end type and calculating TTC for rear-end type. After distinguishing PBs from vehicles in terms of an object length, the rear (bumper) points are estimated based on a slope of every point along its trajectory at each time stamp. This step is further made automated in Stage 2. As shown in FIGURE 38, the black points are estimated rear points along a trajectory with red points as front points. The purple dashed line measures the object length. The object shape is defined as both the front and rear points of an object. The trajectory on the left denotes variations of the object shape along a trajectory; the object shape is separated as front- and rear-point trajectories on the right.

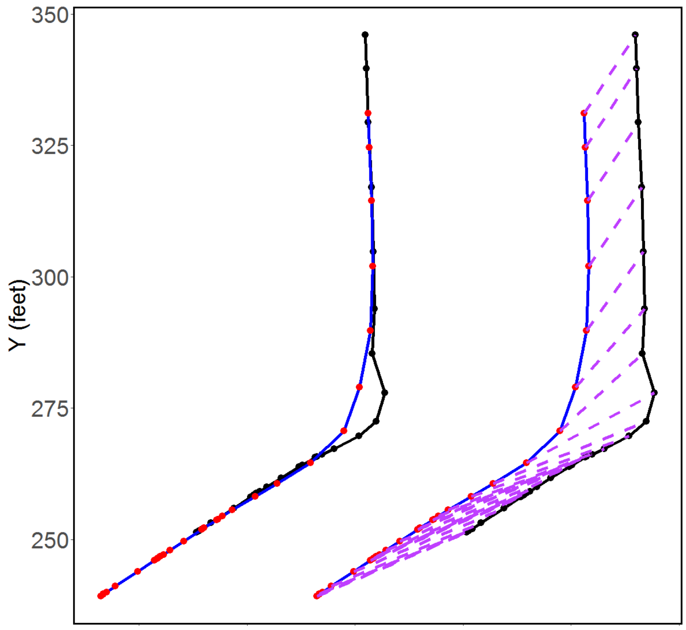

FIGURE 38 Estimation of object shape.

4.1.1.10 Distinguishing Conflicts Based on Conflict Angles

Conflict angles are used to distinguish different types of conflicts. Conflict types were identified by predetermined movement-pair methods in Stage 1. Such methods cannot calculate the conflict angles for each conflicting-vehicle pair; in addition, the method requires a manual configuration of conflicting movement pairs. In Stage 2, any conflict type is classified by calculating conflict angles, which are shown in the FIGURE 39, based on Surrogate Safety Assessment Model (*23*). As shown in FIGURE 39, a rear-end conflict is identified if the conflict angle between two conflicting vehicles is less than 30 degree; a lane-change conflict is identified if the conflict angle between two conflicting vehicles is more than 30 degree and less than 85 degree; and a crossing conflict is identified if the conflict angle between two conflicting vehicles is more than 85 degree and less than 180 degree. Calculating conflict angles is also made automated in Stage 2.

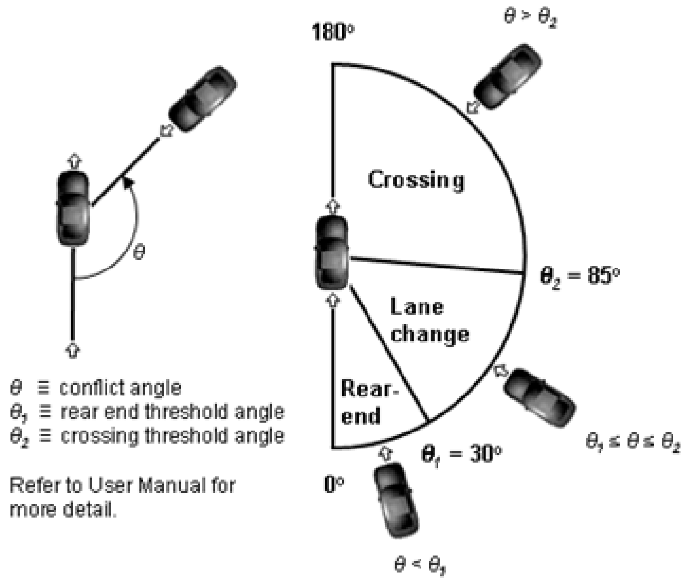

FIGURE 39 Conflict angles between conflicting vehicles (*23*).

4.1.1.11 Surrogate Safety Measurements Based on Conflicts

In some cases, especially those crossing conflicts, i.e., two vehicles may collide at a conflict point rather than on a line, the surrogate safety measure, time-to-collision (TTC) may not be calculated accurately. Such as in **FIGURE *40*** (b), two conflicting vehicles may collide at a specific conflict point, however, with a gap. In such a case, the relative TTC (RTTC) (*32, 33*), i.e., the gap, will be calculated to serve as one of the surrogate safety measures; whereas the TTC cannot be calculated based on its definition (*20*). In **FIGURE *40*** (a), the TTC can be calculated because the conflicting vehicles would collide at the same point if they remain their trajectory and speed unchanged; whereas the RTTC equals zero based on its definition.

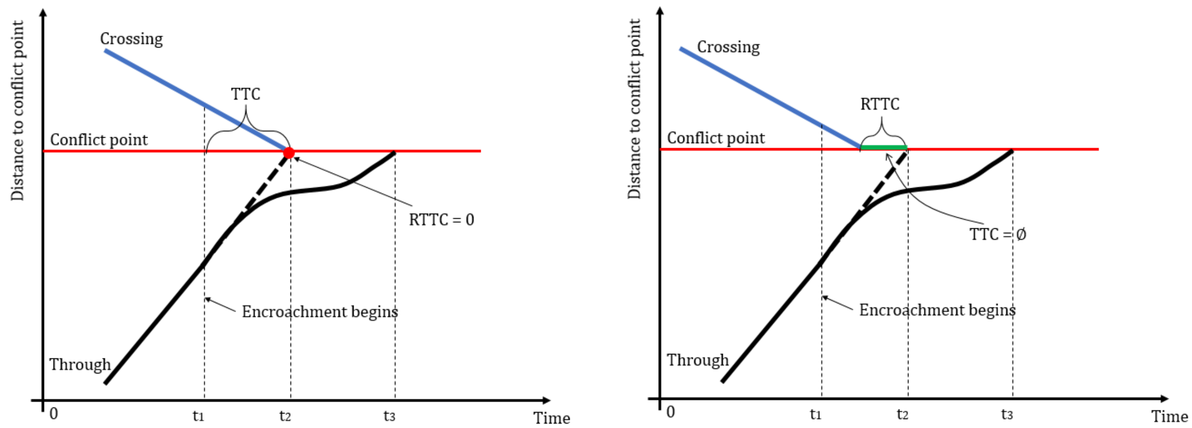

(a) (b)

FIGURE 40 Surrogate safety measurements based on conflicts.

Overall, RTTC is introduced as a new surrogate safety measure in Stage 2, whereas in Stage 1 only TTC was used as the measure. Therefore, if a conflict type of two conflicting objects belongs to rear-end type, only TTC is calculated by a basic method in (*34*). If a conflict type does not belong to the rear-end type, RTTC is calculated, in addition, if RTTC equals zero, TTC will be also calculated.

4.1.2 Automated Application for Any Kind of Intersections

The IPSV can apply to any kind of intersection for detecting conflicts, retrieving speed/volume for any movement, and creating figures based on customized visualization needs. The automated application for any kind of intersection in Stage 2 is realized by configuring lane/movement/stop bar information of any approach in an intersection. Such information can be easily obtained from Google Maps. Boundary coordinate vertices for a base map figure of an intersection can also be obtained from Google Maps for automated visualization needs of any type of conflict-based figure. Such a base map is created based on a main radar sensor's location in the intersection. As shown in FIGURE 41, four radars sensors are located in vicinity of the target intersection, and a main sensor is located in the bottom of the figure. Once the main sensor is determined, the coordinate rotation angle of the other three sensors can be determined from the Google Map based on facing directions of the other three sensors. Similarly, the coordinate displacement of the three sensors to the main sensor can also be determined from the Google Map.

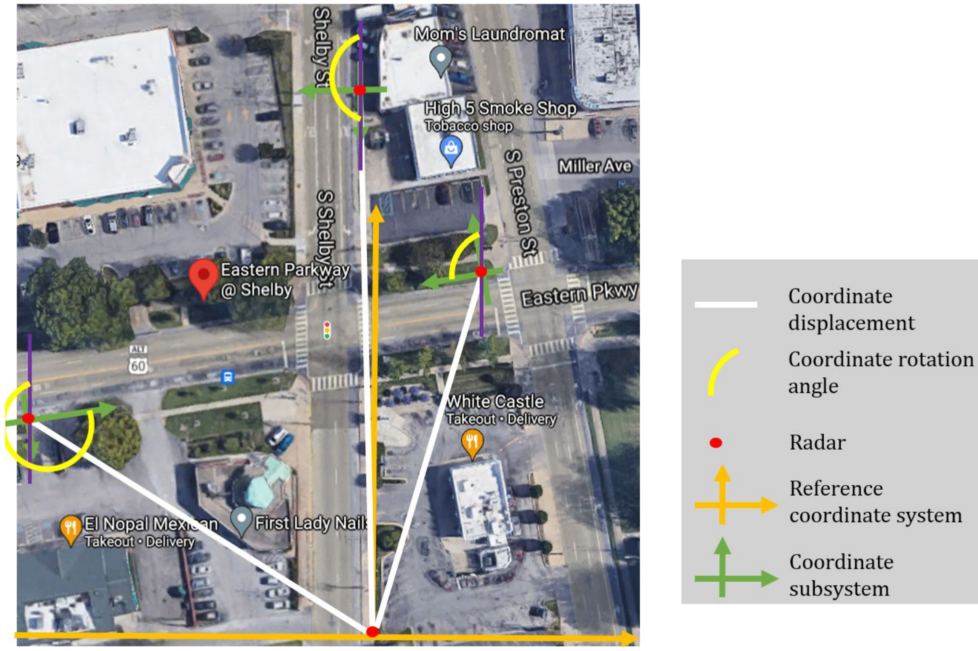

FIGURE 41 Automated data integration and base map creation.

4.2 VALIDATION OF ACCURACY

4.2.1 Data Collection in Stage 2

In Stage 2, the field test intersection was selected as S 24th St @ W Broadway, Louisville. The data collection time was from 14th to 21st, September 2021. The FIGURE 42 gives a presentation of collected trajectories at the intersection.

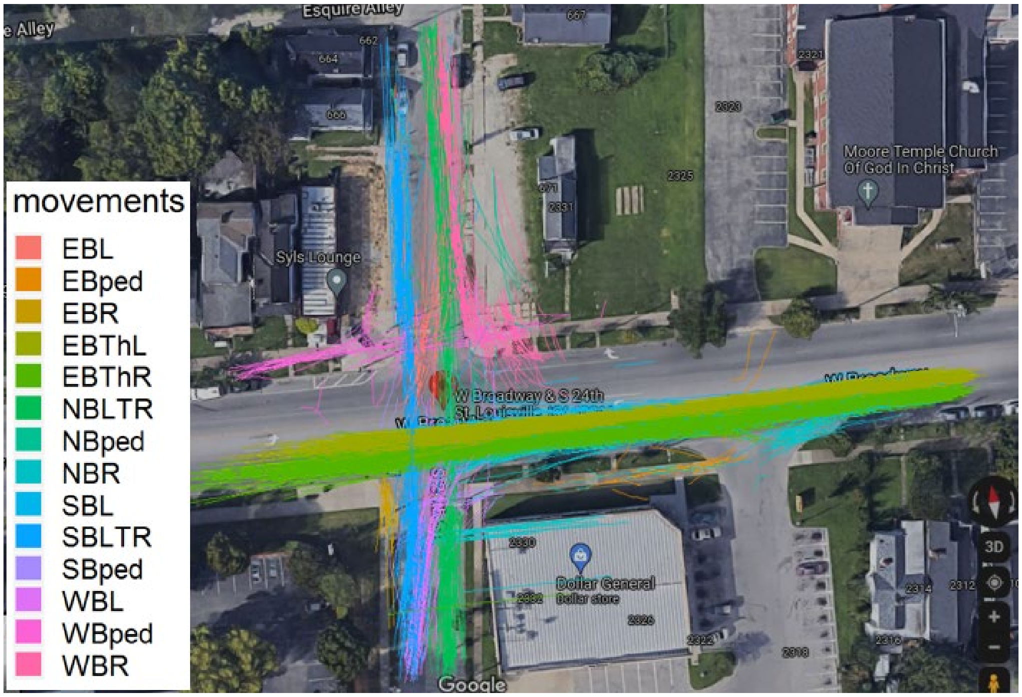

FIGURE 42 Trajectories at 24th St @ Broadway intersection.

4.2.2 Conflict Severity Validation

4.2.2.1 Conflict Severity Validation by TTC

Conflicts detected at this intersection are visualized by rear-end (including lane-changing during a conflict line) type and crossing type (including all others). Rear-end type TTC is also retrieved by a threshold of 1.5 s as in Stage 1; crossing type TTC is retrieved by 4 s. Except rear-end conflict type, all other types are calculated based on RTTC; for these types, a bigger TTC of an object in a conflict pair is retrieved as the TTC for the conflicting pair if both the TTC and RTTC are less than 4 or 1.5 s. As shown in FIGURE 46, **FIGURE *43*** (a) indicates the distribution of the crossing type conflicts with TTC of less than 4 s, and **FIGURE *43*** (b) indicates the distribution of the rear-end and lane-change type conflicts with TTC less than 1.5 s.

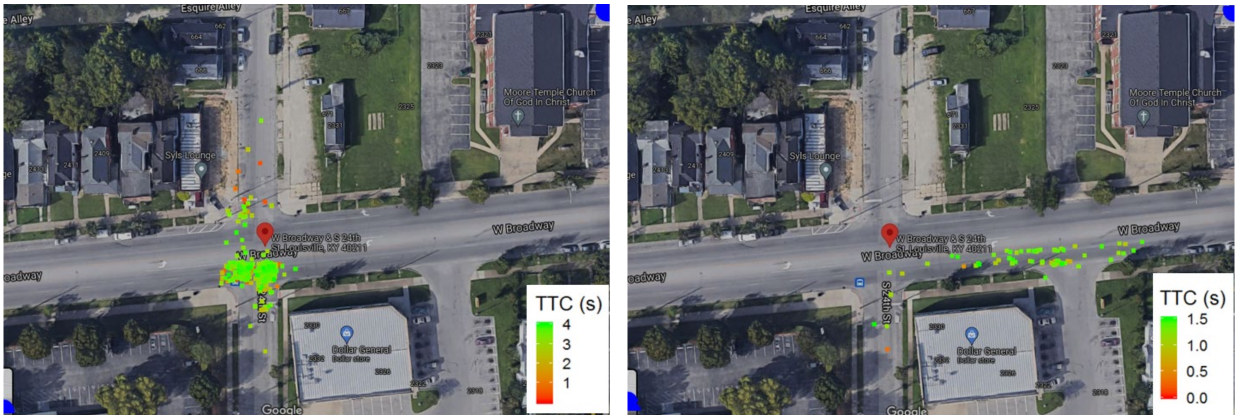

(a) (b)

FIGURE 43 Conflict severity validation by TTC.

4.2.2.2 Conflict Severity Validation by Speed Difference

In Stage 2, speed differences of each conflict pair are used as a measure to identify the severity of the conflicts. The larger the speed difference is, the more likely a conflict event is a crossing conflict; the smaller the speed difference is, the more likely the conflict event is a rear-end conflict. **FIGURE** ***44*** (a) indicates the distribution of the crossing type conflicts with speed different less than 60 ft/s and **FIGURE** ***44*** (b) indicates the distribution of the rear-end/lane-change type conflicts with speed different less than 60 ft/s.

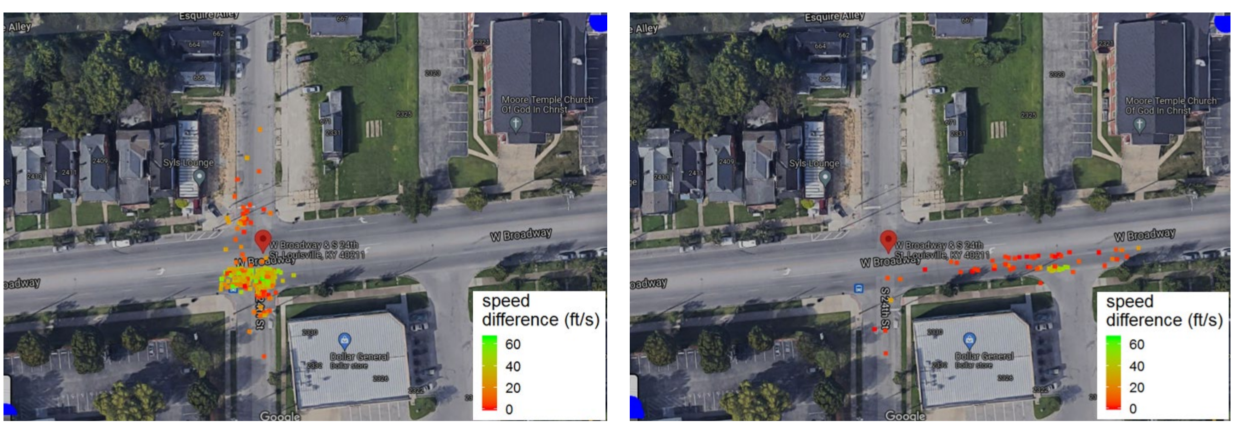

(a) (b)

FIGURE 44 Conflict severity validation by speed difference.

4.2.2.3 Conflict Severity Validation by Conflict Type

For crossing type-based conflicts, the conflict severity is classified by detailed types and movements. The detailed types include sideswipe, left-turn angle, right-angle and pedestrian-to-vehicle types. The FIGURE 45 respectively indicates the type- and movement-based conflict severity validation and distribution at the intersection.

(a) (b)

FIGURE 45 Conflict severity validation by conflict type.

4.2.3 Conflict Quantity Validation

4.2.3.1 Conflict Quantity Validation by Time

Conflict quantities of each conflict type are classified by hours in a day or days in a week to validate the variance of conflicts during the data collection time. As shown in FIGURE 46, different crossing-based conflict types are respectively counted during every hour in a day by conflict quantity.

FIGURE 46 Crossing-based conflict quantity validation by hours.

As shown in FIGURE 47, mostly detected conflict type is the left-turn angle-based. The left-turn angle-based conflict measures a conflict with a conflict angle of more than 30 degrees and less than 85 degrees. The right-angle-based conflict measures a conflict angle of more than degrees and less than 180 degrees. The sideswipe conflict measures all other angle ranges except pedestrian-to-vehicle, left-turn, and right-angle conflicts. The left-turn angle conflicts mostly occur between eastbound through movements and south/northbound through movements at the intersection.

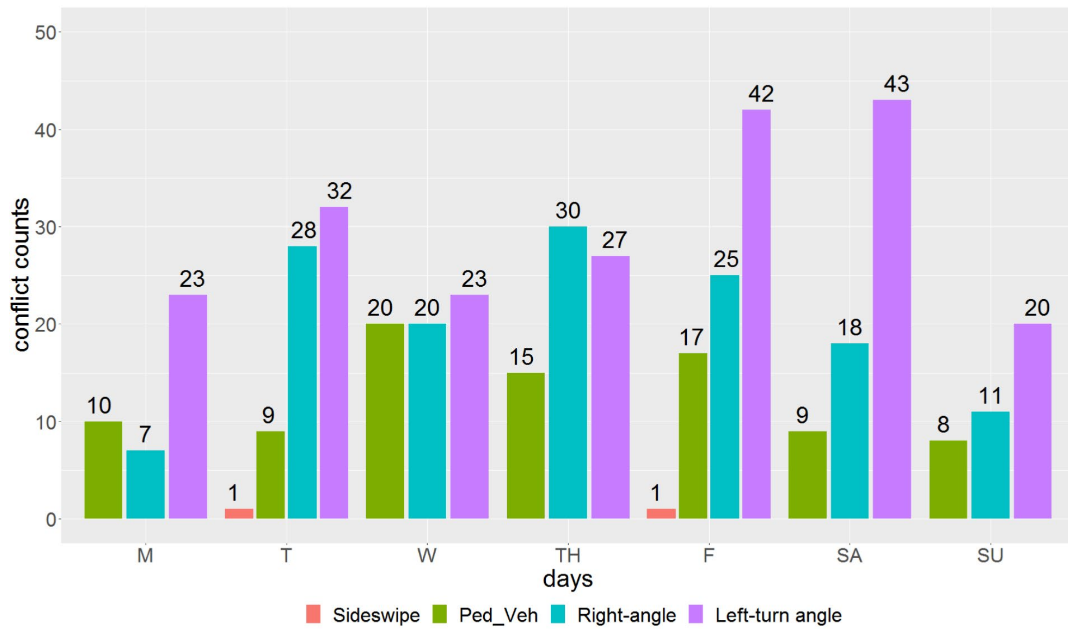

FIGURE 47 Crossing-based conflict quantity validation by days.

As shown in FIGURE 48, rear-end and lane-change conflict types are respectively counted during every hour in a day by conflict quantity.

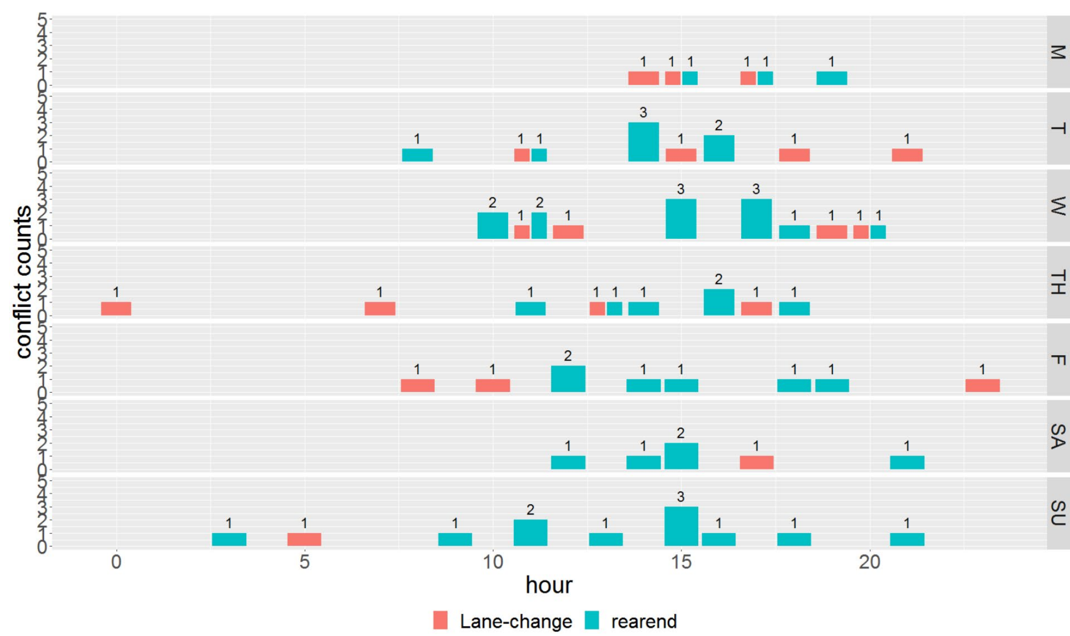

FIGURE 48 Rear-end/lane-change conflict quantity validation by hours.

As shown in FIGURE 49, rear-end conflict type occurs more often than lane-change conflict during conflict line-based events.

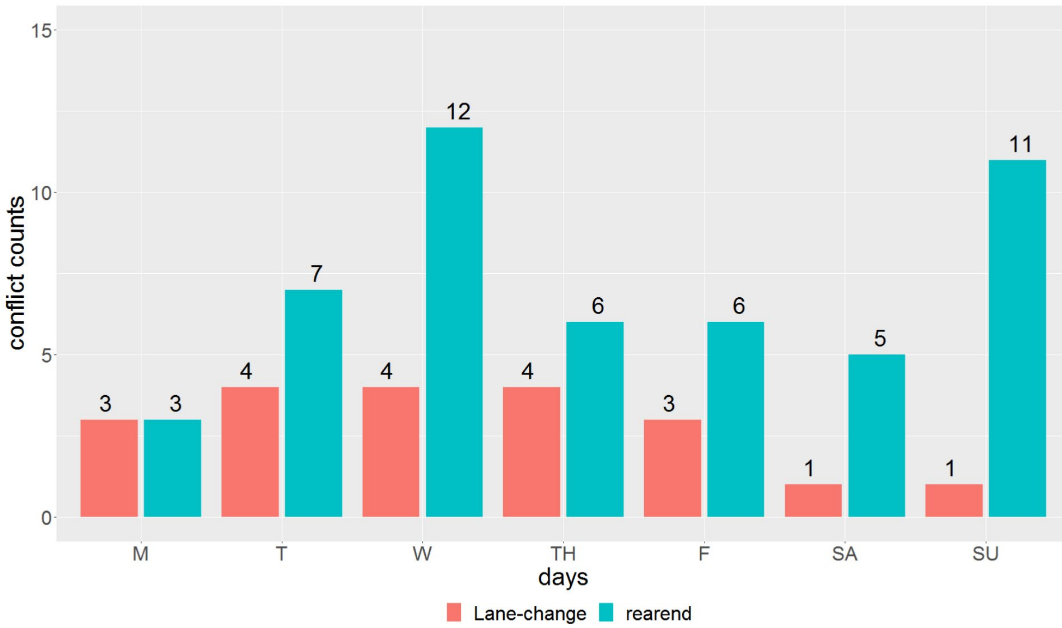

FIGURE 49 Rear-end/lane-change conflict quantity validation by days.

4.2.3.2 Conflict Quantity Validation by TTC Range

Rear-end and lane-change conflict quantity is validated and classified by TTC range under 1.5 s. Crossing conflict quantity is validated and classified by TTC range under 4 s. As shown in FIGURE 50, crossing conflicts with TTC in less than 0.5 s indicate a most dangerous conflict event. Starting from more than 2.5 s, the conflict quantities increase sharply.

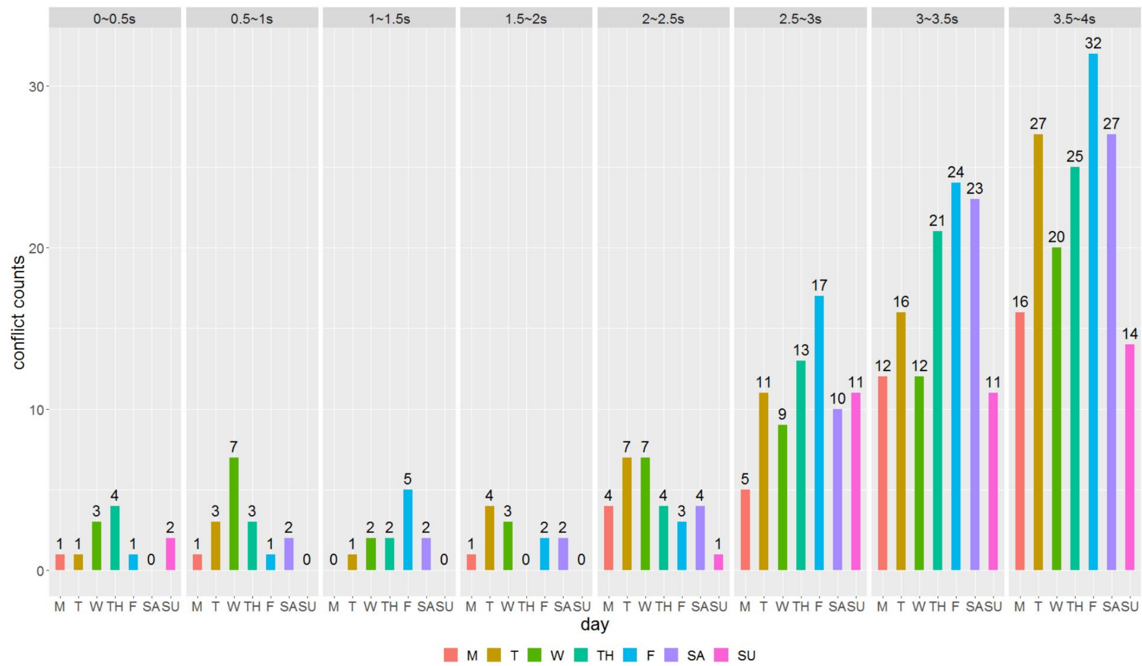

FIGURE 50 Crossing-based conflict quantity validation by TTC range.

As shown in the FIGURE 51, conflicts with TTC of less than 0.5 s occur on Tuesday and Sunday. Conflicts are mostly detected with TTC more than 1 s.

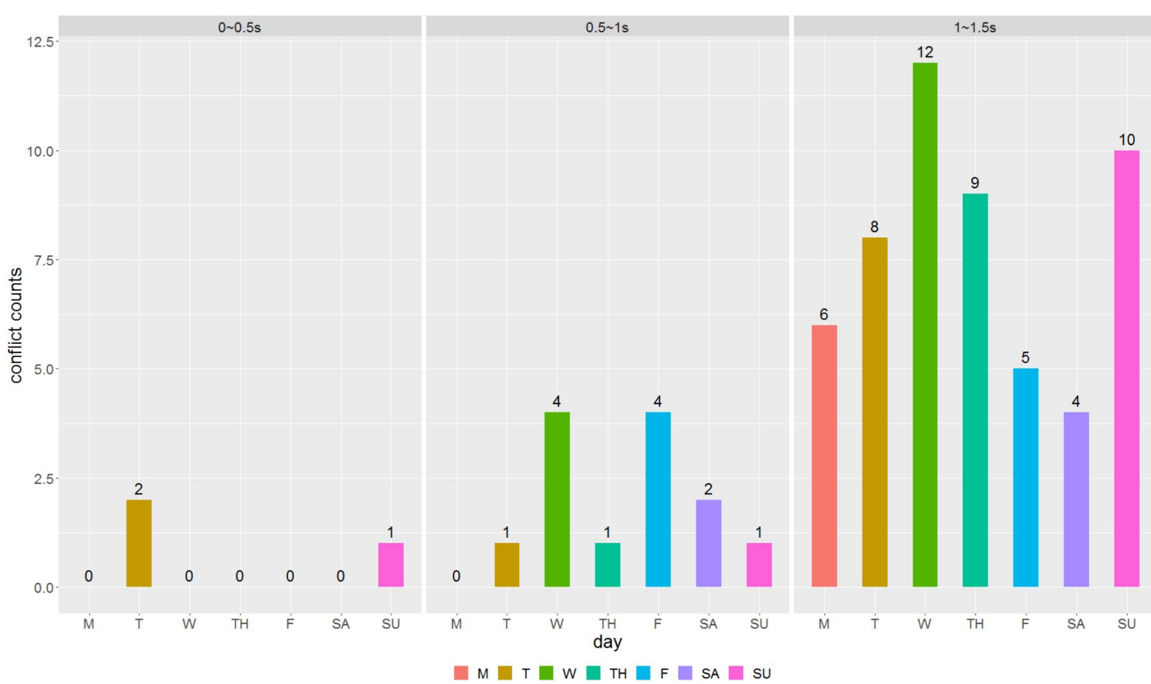

FIGURE 51 Rear-end/lane-change conflict quantity validation by TTC range.

4.2.3.3 Conflict Quantity Validation by Traffic Volume

Each conflict type is also investigated with the variance of both TTC and traffic volume during a week. As shown in FIGURE 52, the same crossing conflict TTC variance pattern was observed in the early morning on Wednesday and Thursday. TTC variance keeps consistent during business hours except on Wednesday.

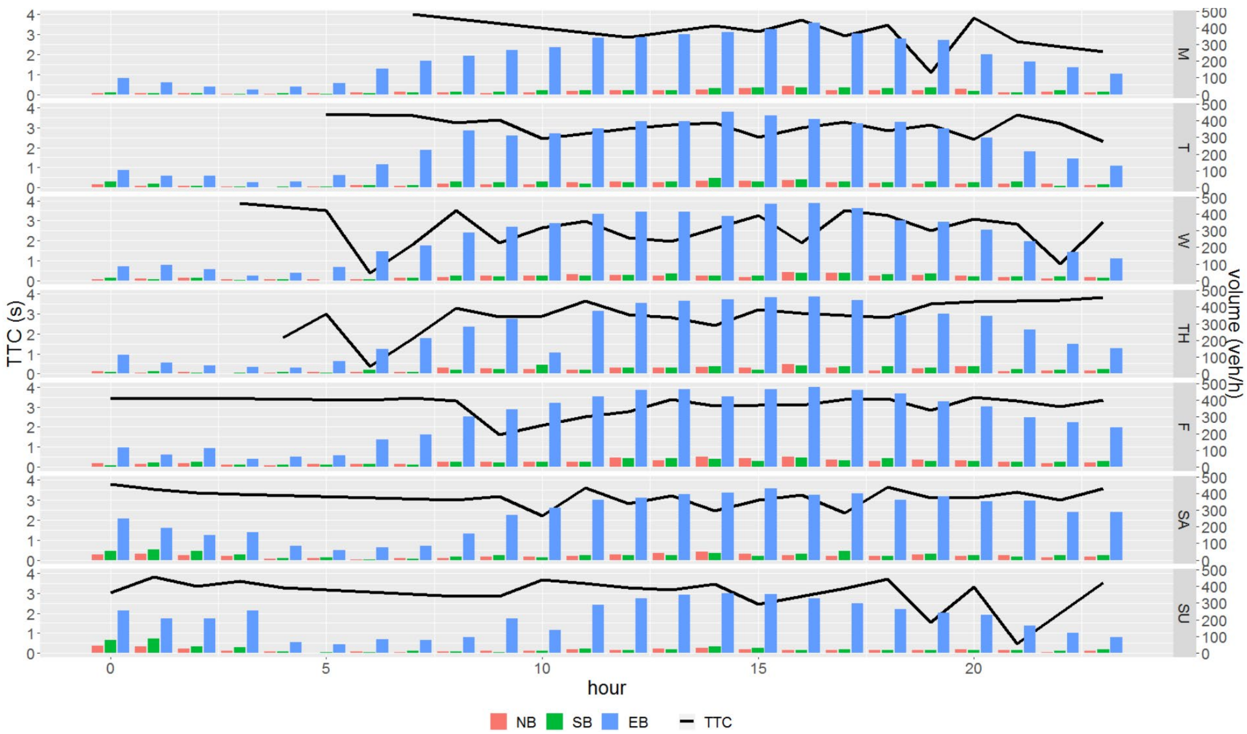

FIGURE 52 Crossing conflicts TTC variance with traffic volume.

As shown in FIGURE 53, no significant TTC variance based on traffic volume is observed due to a limited quantity of rear-end and lane-change conflicts. Similar TTC variance can be observed on Tuesday and Saturday.

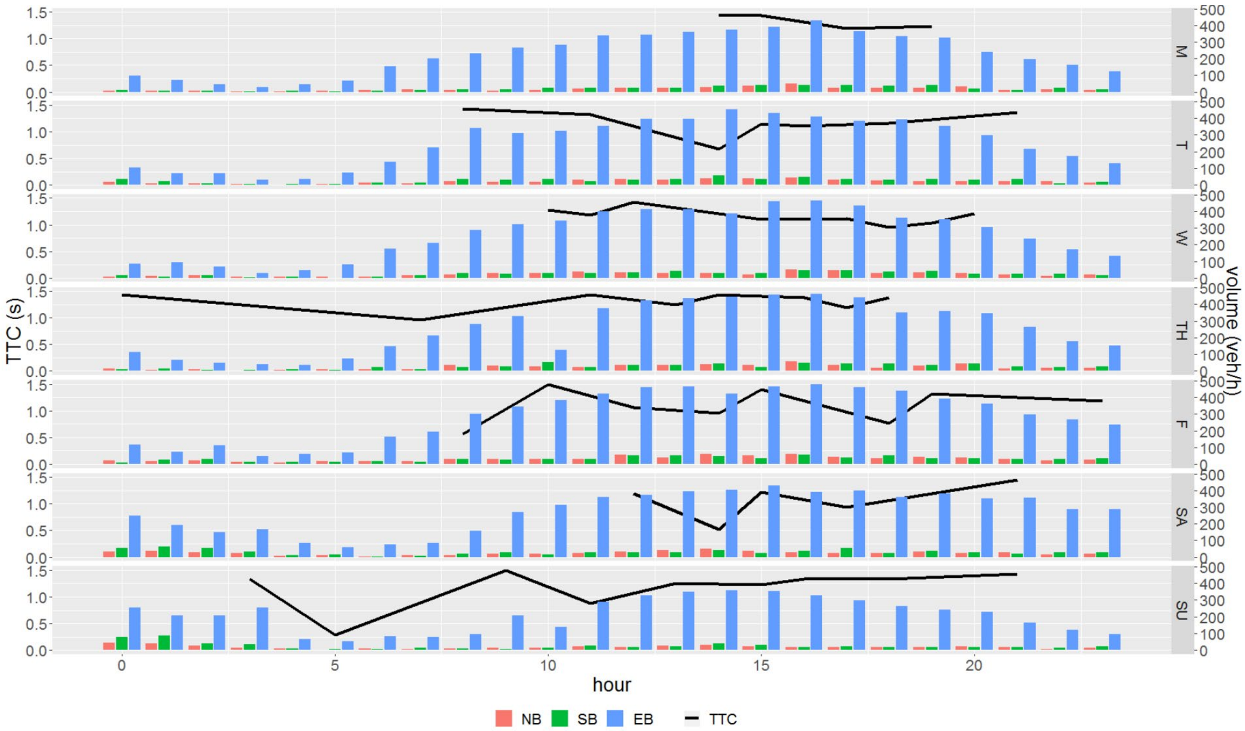

FIGURE 53 Rear-end and lane-change conflict TTC variance with traffic volume.

4.2.4 Validation of Rear-end Conflict Accuracy

It is assumed that a rear-end conflict *can* occur as long as two adjacent vehicles are on the same lane in Stage 1. The trajectories are all snapped onto a lane, on which an average deviation error between points and baseline of the lane is minimal in Stage 1. However, this method would lead to the wrong prediction when a vehicle is making a lane change or the trajectory of the vehicle is not *exactly* on the baseline. Therefore, the trajectories are only smoothened rather than snapped in Stage 2.

When the following vehicle is making a lane change, the conflict would disappear even if the following vehicle is still in the same lane as the leading vehicle. Furthermore, radar positioning error would still exist even after trajectories are smoothened/predicted. These two factors would cause inaccurate TTC values. In addition, most trajectories leave the detection zone of the radar ending at zero speed and lasting up to several minutes. This would increase the false positive rate of conflict identification. This kind of false positive identification is removed in Stage 2.

By sampling from a dataset, rear-end scenarios are detected and classified into three categories: true rear-end scenarios if two conflicting vehicles are in a rear-end conflict event, and false rear-end scenarios caused by lane changing or radar positioning errors. Such sampling result is listed in the following table. Based on **TABLE *2***, the lane change and positioning error scenarios are removed from rear-end conflict calculation in Stage 2. To compare the improvements in rear-end conflict accuracy from Stage 1 to 2, rear-end conflict results from a sample dataset are classified as follows before false conflicts are removed.

TABLE 2 Rear-end scenario analysis.

All	rear-end	lane change	position error
534	409	22	103
Percentage	77%	4%	19%

In Stage 1, all conflicts listed in **TABLE *3*** are counted as rear-end conflict types; whereas in Stage 2, the true negative cases are removed and the false positive cases are classified as lane-change conflict types. Therefore, confusion matrix values under Stages 1 and 2 are calculated as follows.

TABLE 3 Rear-end conflict classification.

All	TP: rear-end	TN: stopping/short travel distance	FP: lane change
77	5	68	4

Based on **TABLE *4***, the TPR decreases from 100% to 80% in Stage 2 because positioning error cases are removed from rear-end conflict identification, however, such cases still lead to inaccurate TTC calculation in Stage 1. The FPR decreases from 100% to 0% in Stage 2 because lane-change cases are separated from rear-end cases.

TABLE 4 Confusion matrix values calculation.

	Stage 2	Stage 1
TPR	$\frac{5}{5+\frac{5}{0.77}*0.19} = 80\%$	$\frac{5}{5+0} = 100\%$

FNR	$\dfrac{\frac{5}{0.77}*0.19}{5+\frac{5}{0.77}*0.19}=20\%$	$\dfrac{0}{5+0}=0\%$
FPR	$\dfrac{0}{68+\frac{5}{0.77}*0.04}=0\%$	$\dfrac{68+4+\frac{5}{0.77}*0.04}{68+4+\frac{5}{0.77}*0.04}=100\%$
TNR	$\dfrac{68+\frac{5}{0.77}*0.04}{68+\frac{5}{0.77}*0.04}=100\%$	$\dfrac{0}{68+4+\frac{5}{0.77}*0.04}=0\%$

4.2.5 Validation of Crossing Conflict Accuracy

When calculating crossing conflicts, any vehicle-to-vehicle and vehicle-to-pedestrian pairs are calculated for a crossing TTC. Therefore, the method of crossing conflict detection in Stage 2 remains the same as in Stage 1. To further validate the crossing conflict accuracy, crossing TTC is calculated respectively based on trajectories and ground truth observation. Four crossing cases are retrieved for validation, which are shown in the FIGURE 54.

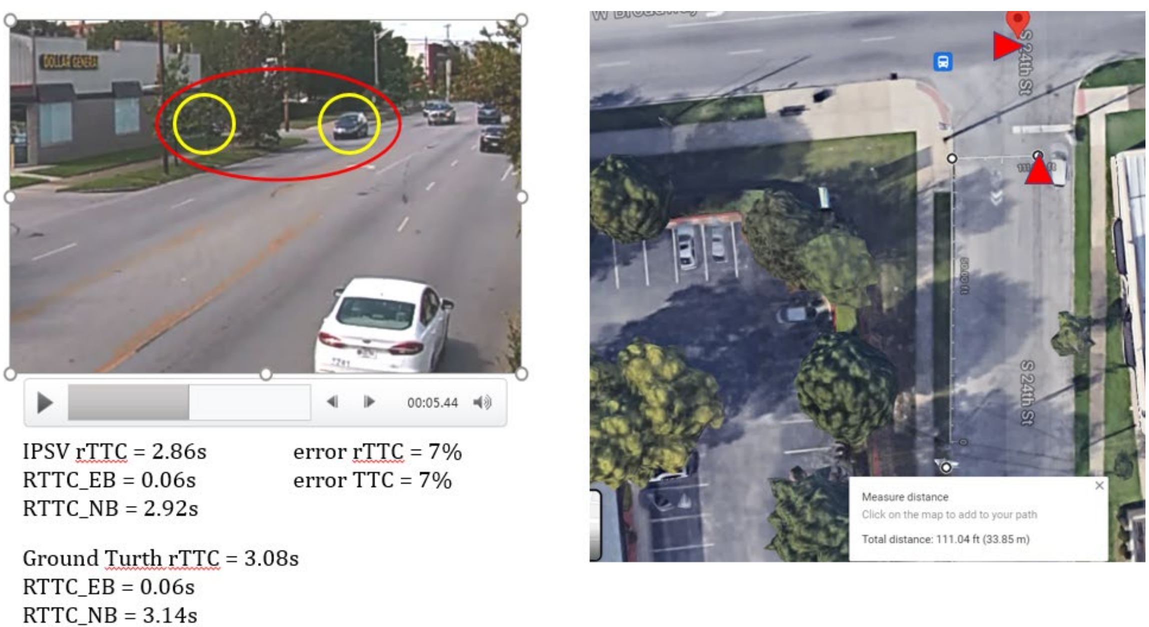

(a)

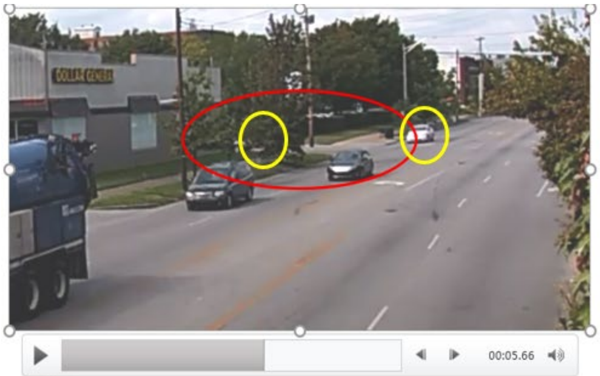

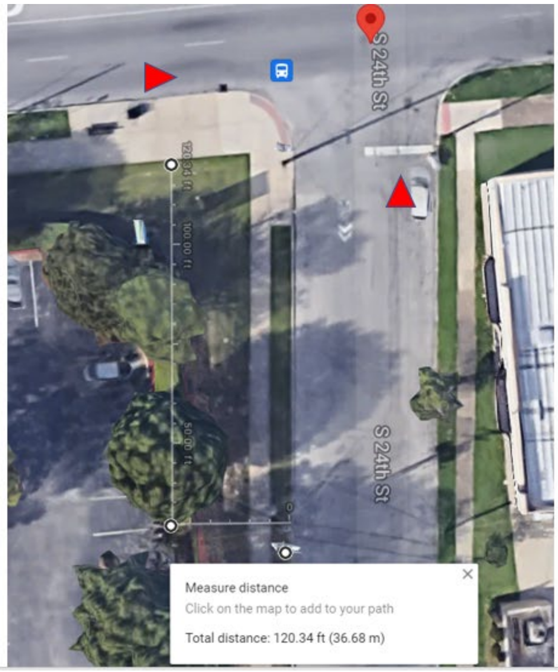

IPSV rTTC = 1.55s
RTTC_EB = 1.37s
RTTC_NB = 2.93s

error rTTC = 12%
error TTC = 7%

Ground Turth rTTC = 1.77s
RTTC_EB = 1.37s
RTTC_NB = 3.14s

(b)

IPSV rTTC = 0.682s
RTTC_ped = 3.366s
RTTC_veh = 2.684s

error rTTC = -0.3%
error TTC = 0.07%

Ground Turth rTTC = 0.680s
RTTC_ped = 3.366s
RTTC_veh = 2.686s

(c)

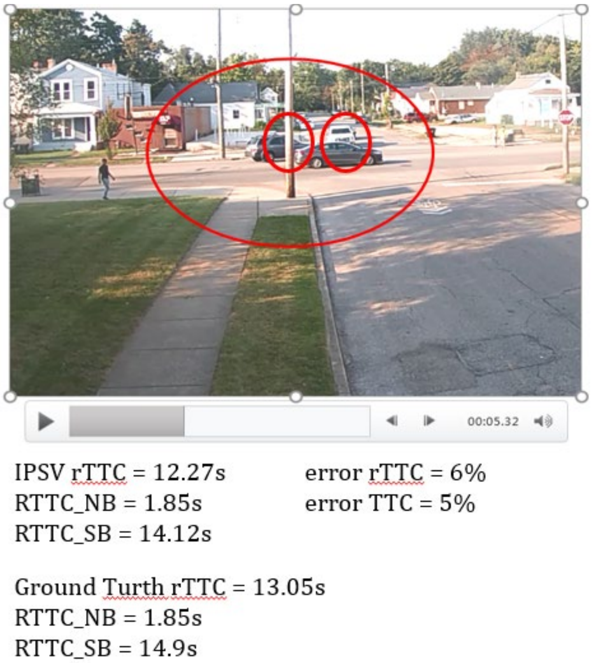

(d)

Figure 54 Validation of crossing conflict accuracy.

The RTTC and TTC of the crossing conflicts are respectively validated through videos and measurements from Google Maps. Based on the above four cases, the average RTTC error rate is 6.2%, and the average TTC error rate is 4.8%, i.e., a crossing TTC calculated by IPSV ranges $[TTC, 1.048 \times TTC]$.

5. PLAN FOR IMPLEMENTATION

5.1 TOOLS FOR IMPLEMENTATION

To facilitate implementing IPSV, the research team has developed an IPSV configuration tool. Figure 55 illustrates the framework of the IPSV configuration and query interface.

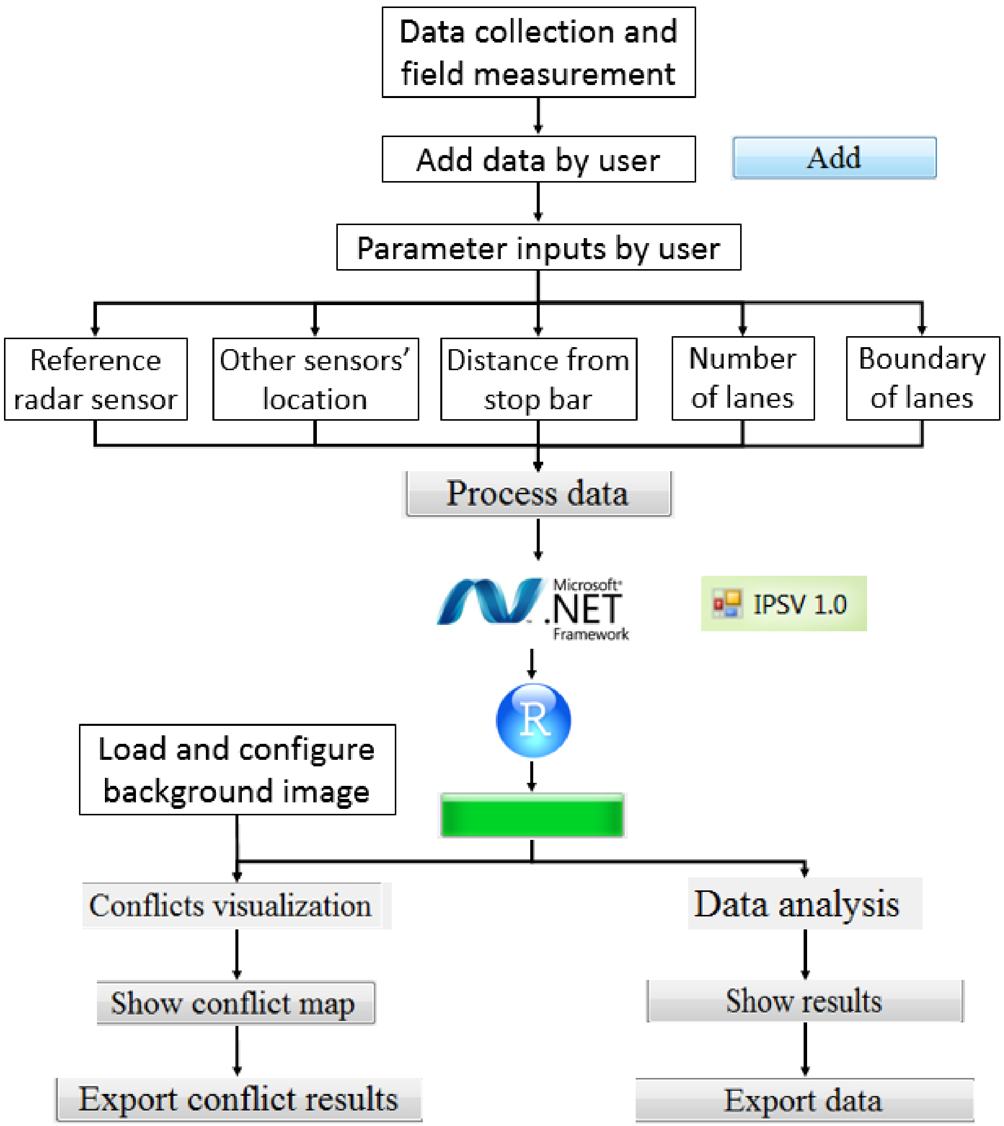

Figure 55 Framework of the IPSV configuration and query tool

Once field data collection is finished, the user can use the interface to configure the data. First, the user will add query data with desired range, i.e., which duration of time on which period of day(s), then click the 'Add' button. The data range input by the user will then be passed to the IPSV interface. This configuration tool is programmed using the .NET framework based on C#; second, the user will input the location info of the main reference radar sensor and other radar sensors. Distance from the stop bar of the oncoming approach of each radar sensor will also be input into the IPSV configuration interface. Similarly, the location information will be received by the IPSV interface after the user clicks the ‘Process data’ button; third, the user needs to load and configure the background image, which is manually retrieved from Google aerial map. The map coordinates need to be configured to reflect the reference radar sensor’s coordinates The tool also helps generate customized queries through the IPSV interface to run R script to map certain traffic conflicts and severities. As shown in Figure 56, the user can also analyze speed or volume by approach or movement under the “operation” section. The user can analyze conflict counts, illegal left turns, etc. under the “safety” section. Similarly, the user can visualize the data analysis results and get the processed data in detail by clicking ‘export data’. For example, in Figure 56, 24-hour data on each day during the whole data collection week is visualized, after the query information is input into the IPSV configuration and query interface. The intersection conflicts and operation data analyses are also visualized in the interface tool.

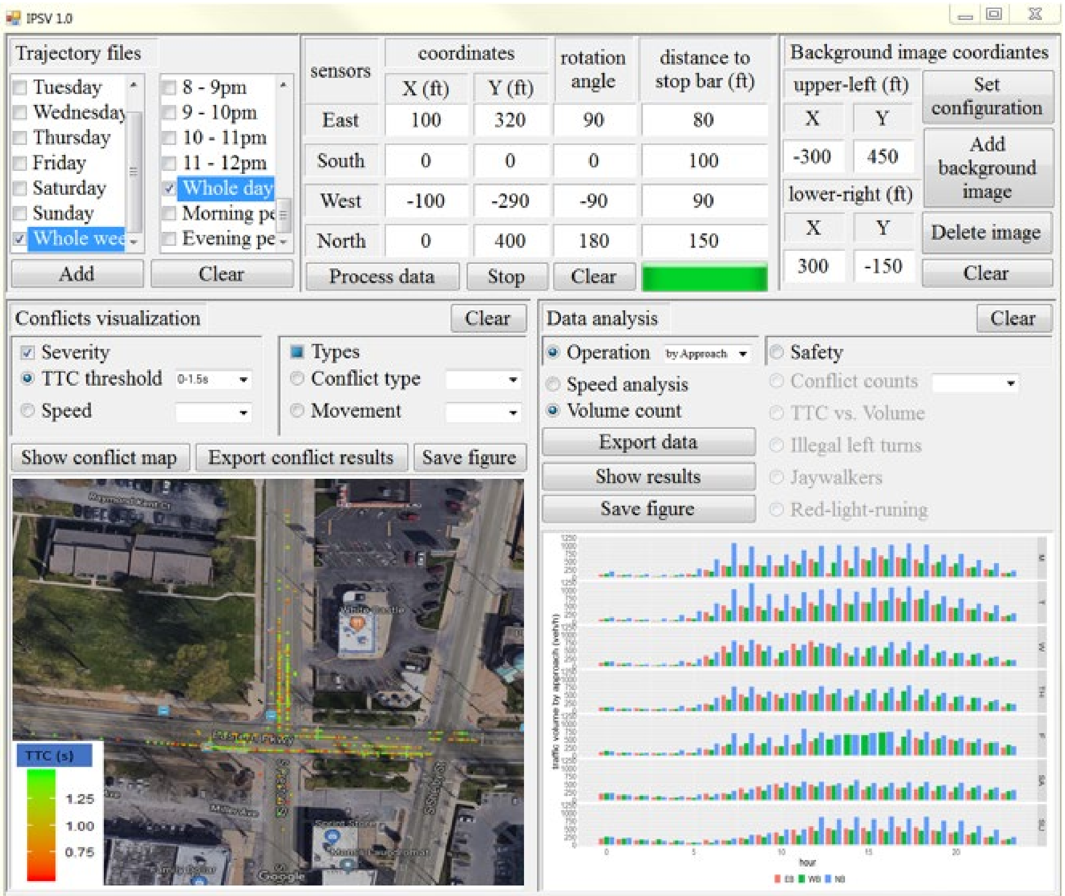

Figure 56 IPSV configuration and query interface with visualization of the results.

The research team also developed a Field Data Collection Manual to facilitate field engineers (state DOT personnel or consultants) to install, calibrate and start the radar data collection at the study site. Figure 57 illustrates a sample page of the field data collection manual.

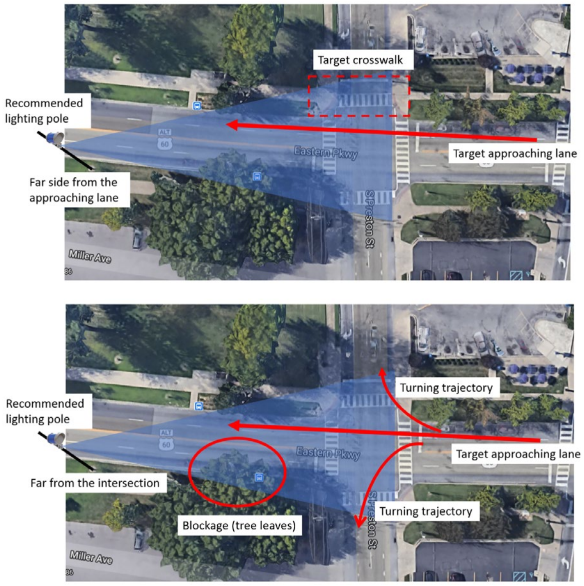

If the trajectories of pedestrians and turning vehicles from certain approach are needed (in terms of one radar sensor) in the safety assessment of the intersection:

1. Confirm candidate lighting poles on Google Map street view
2. Test if the lighting poles can cover crosswalks by geometry tools (a 30-degree detection width from the radar sensor) on the computer
3. Confirm the selected lighting poles exist as where it is at the field as on Google Map
4. Confirm there is not any blockage at front of the radar sensor on one lighting pole, such as tree leaves; otherwise select another candidate lighting pole

Figure 57 Sample IPSV Field Data Collection Manual

5.2 TECHNOLOGY TRANSFER

Throughout this report, a proof-of-concept intersection safety monitoring and visualization tool is developed based on processing radar sensor data in real-time. This tool proactively identifies traffic conflicts in the vicinity of an intersection without passively waiting for a crash occurring. This feature enables state DOTs to measure the safety performance of any intersection and finally decide which intersection of interest for installing safety countermeasure facility, such as rectangular rapid-flashing beacon (RRFB), or other safety or operational upgrade. Overall, some steps for this technology transfer are needed and summarized as follows.

1. Train engineers of state DOTs to efficiently install radar sensors and calibrate and collect trajectory data based on the field data collection manual.
2. Train engineers of state DOTs to operate the IPSV Graphical User Interface (GUI) and obtain needed safety and operational results.
3. Facility the visualization of traffic conflicts at an intersection based on the IPSV GUI for state DOT decision makers and making decisions about any potential upgrades at the intersection.

6. CONCLUSIONS

A proactive intersection safety monitoring and visualization system, IPSV, was developed through the fund from the NCHRP IDEA program. Unlike other safety analysis applications on the current market, the IPSV can be implemented at any kind of intersection for any type of safety and operation analysis under a long-term data collection period. Results obtained from the IPSV can be concluded from the following perspectives:

1. The IPSV is a readily used system that can be commercially deployed by transportation agencies for operational or safety analyses at any kind of intersection. The operational and safety analysis functions are automated and integrated into the IPSV system, along with a user interface for customized queries, analyses, and visualizations.
2. The IPSV provides conflict severity distribution visualization by TTC value, the speed difference between conflicting objects, and any conflict/movement type. From the visualization, more dangerous spots where conflicts occur can be identified at an intersection, i.e., the conflict hot spots can be exactly targeted at a satellite map of the intersection. In addition, the speed difference between conflicting objects can be analyzed along with the hot spots. Conflict-/movement-type based visualization can also help understand what kinds of conflicts the safety issues of the intersection are.
3. The IPSV also provides conflict quantity analyses categorized by time, TTC range, and traffic volume. During different times in a day, the variance of the conflict quantity of different conflict types can be obtained from the system. By setting TTC thresholds for different conflict types, quantities of conflicts that fall in different TTC ranges can be easily summarized. Additionally, the TTC variance can also be investigated along with the variance of the traffic volume during a day.
4. To validate the conflict results obtained from IPSV, ground truths found in videos are manually compared with corresponding conflicts in terms of severity and quantity. It is found that the conflict quantity achieves an 80% true positive rate and a 100% true negative rate after upgrading the IPSV in Stage 2. It is also found that the conflict severity achieves an average 95.2% accuracy in terms of the TTC of a conflict.
5. The IPSV works as a fundamental platform for identifying safety issues of both the signalized and stop-controlled intersections. Two signalized intersections were selected as the test intersections in Stage 1, where the number of conflicts of rear-end is more than

the crossing type and illegal left turn and red light running were observed. A stop-controlled intersection was selected in Stage 2, where number of conflicts of crossing type is more than rear-end type, and conflicts of pedestrian-to-vehicle are mostly observed. Overall, regarding different types of intersections, the IPSV can identify corresponding safety problems. The IPSV can facilitate transportation agencies in making decisions on which intersections need to be improved in terms of safety based on quantitative performance measures (conflicts and their severities) by the IPSV.

7. FUTURE WORK

During the development of the IPSV and deploying the system at an intersection, several challenges were found, and potential solutions are provided for the potential future proof-of-concept project.

The first challenge that is learned from the development in Stage 1 is that positioning errors caused by windy conditions can lead to less accurate TTC measurements and false or missed conflict detections. In general, positioning errors occur for any types of sensors deployed for data collection, including GPS, Lidar, and video cameras. Such positioning errors, however, can be mostly eliminated by post-processing algorithms. Such post-processing algorithms have been developed and implemented in Stage 2 of this project and have improved the accuracy. During the IPSV development in Stage 2, detected trajectories are smoothed and extrapolated, however, there still exists a few trajectories (very rare) with sharp slope changes, which are unrealistic on the road. This sharp slope change may be caused by disruptions to radar signals on tracking an object. Since such sharp slope changes are unrealistic, those trajectories with the characters can be further projected to either a through or turning movement without considering those trajectory points with sharp slope change.

The second challenge comes from the calibration of the trajectory of IPSV with the trajectory in the ground truth. It costs labor work to obtain ground truth trajectories from videos. Because the greater number of ground truth is retrieved, the more accurate the calibration is and so is the conflict severity. More labor calibrations are recommended for better conflict detection results. To facilitate calibration, this project has developed a field installation/calibration guidebook, which can be directly used in future proof-of-concept implementation project.

The third challenge arises in radar sensors' field data collection and calibration. For a radar sensor that is mounted on a lighting pole, it is important to avoid any blockage of view within the detection zone of the radar sensor, which is also noted in the field installation/calibration guidebook; otherwise, the data can become unreliable. In addition, a continuous trajectory rather than a discrete trajectory is recommended for visualization in the field when doing the radar sensor angle calibration. Especially, for a scenario where the trajectories of pedestrians are the main targets, probe pedestrian data needed to be tested in the calibration process to make sure that the radar sensor can track the trajectories of pedestrians because the pedestrians’ trajectories can be lost due to distance or blockage of view.

REFERENCES

1. Songchitruksa, P. and A.P. Tarko, *The extreme value theory approach to safety estimation.* Accident Analysis & Prevention, 2006. **38**(4): p. 811-822.
2. Sayed, T. and S. Zein, *Traffic conflict standards for intersections.* Transportation Planning and Technology, 1999. **22**(4): p. 309-323.
3. Amundsen, F. and C. Hyden, *Proceedings of first workshop on traffic conflicts.* Oslo, TTI, Oslo, Norway and LTH Lund, Sweden, 1977.
4. Noyce, D., et al., *Automated Turning Movement Counts for Shared Lanes Using Existing Vehicle Detection Infrastructure*, in *NCHRP IDEA Project 177*. 2016.
5. Santiago-Chaparro, K.R. and D.A. Noyce, *Expanding the Capabilities of Radar-Based Vehicle Detection Systems: Noise Characterization and Removal Procedures.* Transportation Research Record, 2019: p. 0361198119852607.
6. Shankwitz, C.R., et al., *Intersection assistance system and method*. 2007, Google Patents.
7. Noyce, D.A., et al., *Turning Movement Counts on Shared Lanes: Prototype Development and Analysis Procedures*, in *NCHRP IDEA Project 198*. 2019.
8. Ma, M. and Z. Li, *A Proactive Approach for Intersection Safety Visualization based on Real-Time Radar Sensor Data.* Transportation Research Board 98th Annual Meeting, 2019. **No.19-01628**.
9. Misener, J., et al., *California Intersection Decision Support: A Systems Approach to Achieve Nationally Interoperable Solutions II*, in *UCB-ITS-PRR-2007-1*. 2007, California Partners for Advanced Transit and Highways.
10. Sacchi, E. and T. Sayed, *Conflict-based safety performance functions for predicting traffic collisions by type.* Transportation Research Record, 2016. **2583**(1): p. 50-55.
11. Zheng, L. and T. Sayed, *Comparison of Traffic Conflict Indicators for Crash Estimation using Peak Over Threshold Approach.* Transportation Research Record, 2019: p. 0361198119841556.
12. Zheng, L. and T. Sayed, *Bayesian hierarchical modeling of traffic conflict extremes for crash estimation: A non-stationary peak over threshold approach.* Analytic Methods in Accident Research, 2019. **24**: p. 100106.

13. Zheng, L. and T. Sayed, *A full Bayes approach for traffic conflict-based before–after safety evaluation using extreme value theory.* Accident Analysis & Prevention, 2019. **131**: p. 308-315.
14. Zheng, L. and T. Sayed, *From univariate to bivariate extreme value models: Approaches to integrate traffic conflict indicators for crash estimation.* Transportation Research Part C: Emerging Technologies, 2019. **103**: p. 211-225.
15. Zheng, L., T. Sayed, and M. Essa, *Validating the bivariate extreme value modeling approach for road safety estimation with different traffic conflict indicators.* Accident Analysis & Prevention, 2019. **123**: p. 314-323.
16. Jahangiri, A., et al., *Developing a Computer Vision-Based Decision Support System for Intersection Safety Monitoring and Assessment of Vulnerable Road Users*. 2020, Mineta Transportation Institute.
17. Wu, Y., et al., *Automated Safety Diagnosis Based on Unmanned Aerial Vehicle Video and Deep Learning Algorithm.* Transportation Research Record, 2020: p. 0361198120925808.
18. Wu, J., Y. Zhang, and H. Xu, *A novel skateboarder-related near-crash identification method with roadside LiDAR data.* Accident Analysis & Prevention, 2020. **137**: p. 105438.
19. Wu, J., et al., *A novel method of vehicle-pedestrian near-crash identification with roadside LiDAR data.* Accident Analysis & Prevention, 2018. **121**: p. 238-249.
20. Gettman, D. and L. Head, *Surrogate safety measures from traffic simulation models.* Transportation Research Record, 2003. **1840**(1): p. 104-115.
21. Van Der Horst, R. and J. Hogema, *Time-to-collision and collision avoidance systems*, in *6th ICTCT workshop Salzburg*. 1993.
22. Essa, M. and T. Sayed, *Full Bayesian conflict-based models for real time safety evaluation of signalized intersections.* Accident Analysis & Prevention, 2019. **129**: p. 367-381.
23. Gettman, D., et al., *Surrogate safety assessment model and validation: Final Report*. 2008, United States. Federal Highway Administration. Office of Safety Research and Development.
24. Hirst, S., *The format and presentation of collision warnings.* Ergonomics and safety of intelligent driver interfaces, 1997: p. 203.
25. Hogema, J. and W. Janssen, *Effects of intelligent cruise control on driving behavior: a simulator study.* TNO Human Factors, Soesterberg, The Netherlands., 1996.

26. Tachet, R., et al., *Revisiting street intersections using slot-based systems.* PloS one, 2016. **11**(3): p. e0149607.
27. Ozbay, K., et al., *Derivation and validation of new simulation-based surrogate safety measure.* Transportation Research Record, 2008. **2083**(1): p. 105-113.
28. Li, Z., et al., *Automated identification and extraction of horizontal curve information from geographic information system roadway maps.* Transportation research record, 2012. **2291**(1): p. 80-92.
29. Cleveland, W.S., E. Grosse, and W.M. Shyu, *Local regression models*, in *Statistical models in S*. 2017, Routledge. p. 309-376.
30. Cleveland, W.S. and C. Loader, *Smoothing by local regression: Principles and methods*, in *Statistical theory and computational aspects of smoothing*. 1996, Springer. p. 10-49.
31. Hartigan, J.A. and M.A. Wong, *Algorithm AS 136: A k-means clustering algorithm.* Journal of the royal statistical society. series c (applied statistics), 1979. **28**(1): p. 100-108.
32. Zhang, Y., et al., *Pedestrian safety analysis in mixed traffic conditions using video data.* IEEE Transactions on Intelligent Transportation Systems, 2012. **13**(4): p. 1832-1844.
33. Chen, P., et al., *Surrogate safety analysis of pedestrian-vehicle conflict at intersections using unmanned aerial vehicle videos.* Journal of advanced transportation, 2017. **2017**.
34. Essa, M. and T. Sayed, *Traffic conflict models to evaluate the safety of signalized intersections at the cycle level.* Transportation research part C: emerging technologies, 2018. **89**: p. 289-302.
35. Sharma A., Bullock D. M., and Peeta, S. *Recasting Dilemma Zone Design as a Marginal Cost-Benefits Problem.* Transportation Research Record No. 2035, Transportation Research Board of the National Academies, Washington, D.C., 2007. 88-96.

Research Results

Real-Time Proactive Intersection Safety Monitoring and Visualization

A proactive intersection safety monitoring and visualization tool that can be implemented at any kind of intersection

Program Steering Committee:
NCHRP IDEA Program Committee

July 2022

Title:
A Real-Time Proactive Intersection Safety Monitoring and Visualization System Based on Radar Sensor Data

Project Number:
NCHRP IDEA 217

Start Date: July 1, 2019

Completion Date: June 30, 2022

Product Category:
New or improved tool

Principal Investigator:
Li, Zhixia, Associate Professor
University of Louisville
richard.li@louisville.edu
502-852-2307

WHAT WAS THE NEED?

Monitoring and visualization of traffic safety at intersections is an essential step leading to the ultimate development of safety treatment solutions. Traditional visualization methods include intersection collision diagrams and GIS-based intersection crash hot spot maps. As all these methods are based on historical crash data, the visualizations cannot be created until sufficient crash data are collected, which may take years and is at the cost of potential injuries and fatalities. Such ***reactive*** methods hinder transportation agencies from effectively addressing intersection safety issues. Aiming to enhance safety more effectively and efficiently, transportation agencies have begun monitoring traffic flow, collecting traffic data, and conducting safety analyses by using ***proactive*** roadside sensing technologies for decades. These sensing technologies mainly consist of radar sensors, Lidar, and video cameras. However, those safety analyses at an intersection are restricted by a limited data collection time or specific conflict types in a specific traffic scenario. Consistent data collection requires consistent power supplies and/or manual operations and maintenance. In addition, a data processing algorithm in a safety analysis system is developed for only a specific conflict scenario. These restrictions prevent transportation agencies from widely deploying safety applications at any targeted intersection for short-term or long-term safety monitoring.

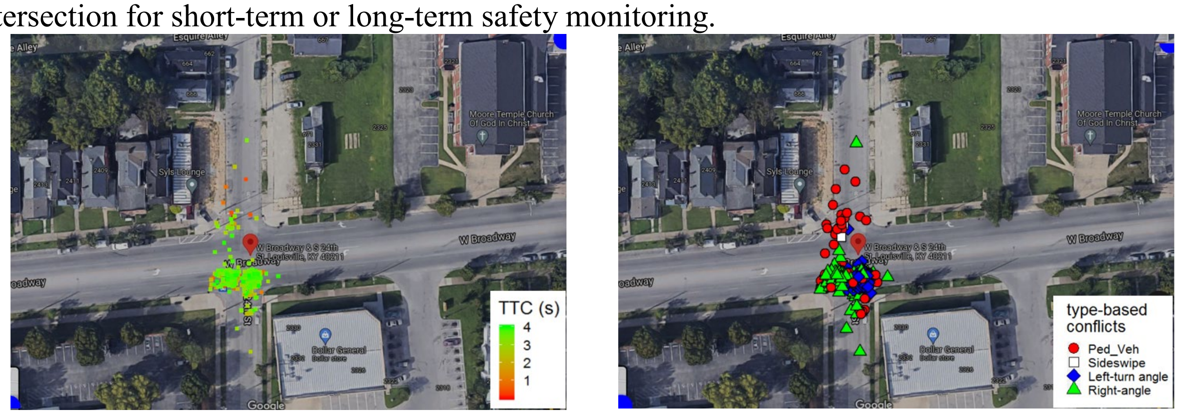

Proactive intersection safety monitoring and visualization on a satellite map

WHAT WAS OUR GOAL?

This IDEA product aimed to develop a **p**roactive **i**ntersection **s**afety monitoring and **v**isualization system (**IPSV**) that can be implemented at any kind of intersection for any type of safety and operation analysis under a long-term data collection period.

WHAT DID WE DO?

First, in contrast to other traffic detection products, such as using video cameras, drones, or Lidar sensors, the IPSV employs a 24GHz Microwave Doppler radar sensor, which can track all detected approaching vehicles and pedestrians' trajectories with update frequency up to 0.3 s/object. Second, based on the vehicle trajectory data, the IPSV calculates time-to-collision (TTC) and detects all possible traffic conflicts at the intersection. These conflict types include rear-end/lane-change/left-turn angle/right-angle/sideswipe/pedestrian-to-vehicle conflicts. Finally, two field data collections were conducted with assistance from the Kentucky Transportation Cabinet (KYTC) to validate the accuracy of the IPSV.

WHAT WAS THE OUTCOME?

An application interface was developed along with the IPSV for users to configure IPSV, and run queries and visualizations. IPSV was validated at both signalized and unsignalized intersections. The improved IPSV system in Stage 2 achieves a high traffic conflict severity detection accuracy with an average 4.8% error rate. The system also achieves an 80% true positive rate and a 100% true negative rate for conflict quantity detection. The results are validated through manual comparisons of ground truth found in videos based on field-collected traffic data.

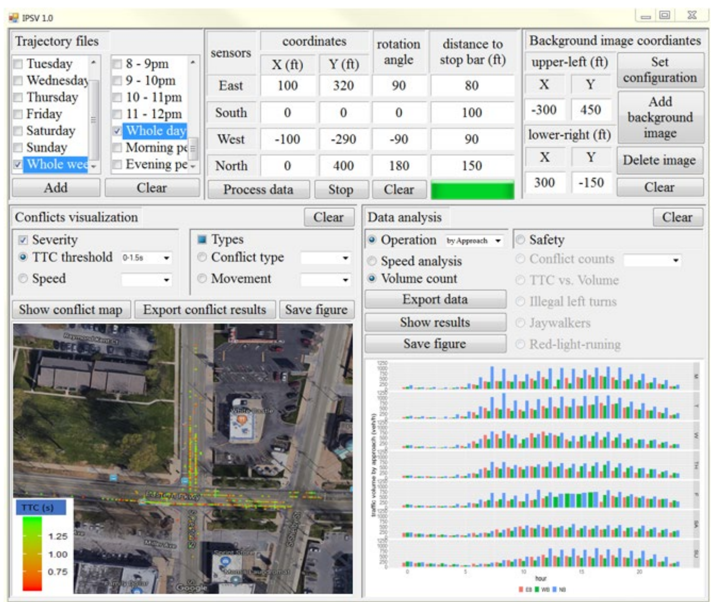

IPSV graphical user interface

WHAT IS THE BENEFIT?

The IPSV provides a cost-effective method to quickly evaluate safety treatment effectiveness for an intersection without the need of waiting crashes to happen; complements the crash data to help transportation agencies and local governments better understand the safety issues at an intersection with traffic conflicts data collected; recognizes wide ranges of road users including vehicles, bicyclists and pedestrians via an explainable feature-based algorithm; detects traffic anomaly consisting of detecting illegal left-turns, jaywalkers, and red-light-runners in any desired observation period; visualizes conflicts severity and quantity straightforwardly with the identifiers of TTC, vehicle speed, movements or conflict types; applies to any type/number/geometry shape of lanes of an approach at an intersection by an automated and integrated system; performs real-time feedback about target intersection safety issues with consecutive 24/7 traffic monitoring. Furthermore, a data collection manual and a series of tutorial videos are created for deploying the IPSV system at an intersection. A system manual is readily utilized for transportation agencies to widely deploy the IPSV at more targeted intersections.

LEARN MORE

To view the complete report from https://engineering.louisville.edu/research/centersinstitutes/cti/